HYDRODYNAMIC ASPECTS OF FISH OLFACTION

Jonathan P. L. Cox

Department of Chemistry, University of Bath, Bath BA2 7AY, UK

j.p.l.cox@bath.ac.uk

Tel. +44 1 225 386548
Fax +44 1 225 386231

SUMMARY

Flow into and around the olfactory chamber of a fish determines how odorant from the fish's immediate environment is transported to the sensory surface (olfactory epithelium) lining the chamber. Diffusion times in water are long, even over comparatively short distances (millimetres). Therefore transport from the external environment to the olfactory epithelium must be controlled by processes that rely on convection (*i.e.* the bulk flow of fluid). These include the beating of cilia lining the olfactory chamber and the relatively inexpensive pumping action of accessory sacs. Flow through the chamber may also be induced by an external flow. Flow over the olfactory epithelium appears to be laminar. Odorant transfer to the olfactory epithelium may be facilitated in several ways: if the olfactory organs are mounted on stalks that penetrate the boundary layer; by the steep velocity gradients generated by beating cilia; by devices that deflect flow into the olfactory chamber; by parallel arrays of olfactory lamellae; by mechanical agitation of the chamber (or olfactory stalks); and by vortices. Overall, however, our knowledge of the hydrodynamics of fish olfaction is far from complete. Several areas of future research are outlined.

Keywords: Fish, olfaction, hydrodynamics, ventilation

1. INTRODUCTION

The first step in fish olfaction is the transport of odorants (*e.g.* amino acids, steroids and prostaglandins) from the external environment to the sensory surface of the olfactory organ. Understanding this step, which is underpinned by hydrodynamic processes, is therefore of fundamental importance, and would complement studies on the anatomy of the olfactory organ (Zeiske *et al.* 1992), the physiology of the olfactory system (*e.g.* Nikonov *et al.* 2005; Hamdani & Døving 2007), and the olfactory behaviour of fish (*e.g.* Pohlmann *et al.* 2001), in addition to studies on the ultrastructure of the olfactory sensory surface (Yamamoto 1982; Hansen & Zielinski 2005) and the cloning and expression of odorant receptor genes (Alioto & Ngai 2005, and references therein).

The purpose of this article is to highlight several hydrodynamic aspects of fish olfaction. Very little work has been done in this area. Indeed, there have been only two detailed studies, one by Kux, Zeiske and colleagues (Kux *et al.* 1977, 1978, 1988), and one by Nevitt (1991). The article will develop some ideas mentioned in passing in the literature, including the effect of boundary layers on fish olfaction, how external flows might be harnessed to assist in ventilating the olfactory organ, and the nature of the flow over the sensory region. It will also introduce some new ideas, including how vortices in and around the olfactory organ might assist in the detection of odorants.

In developing or formulating these ideas, it has been necessary to perform several calculations based on anatomical measurements on a number of different species of fish. These calculations are detailed in Appendix A.

Readers not familiar with fluid dynamics are referred to Massey (1989) and Vogel (1994). A general overview of fluid dynamics in relation to animal (and artificial) noses can be found in Settles (2005).

On first mention, a particular species of fish is referred to by its English common name followed by its current scientific name. Quite often the scientific name of a fish

has changed over the course of time (or has been misrepresented) and thus its scientific name given in a particular reference may not be its current scientific name. Species whose names currently differ from those given in cited references are listed in Appendix B. If mentioned again, the fish is referred to only by its English common name. Current scientific names are taken from the California Academy of Sciences's *Catalog of Fishes* (http://www.calacademy.org/RESEARCH/ichthyology/catalog/fishcatsearch.html). English common names are generally from FishBase (http://www.fishbase.org/search.php). Other types of classification (orders, families *etc.*) are according to Nelson (1994).

2. THE OLFACTORY ORGANS OF FISH

The olfactory organs of fish are often inconspicuous. Typically they occur as a pair of chambers placed symmetrically on the head, lying just beneath its dorsal surface and just in front of the eyes (figure 1) (for a review, see Zeiske *et al.* 1992). Two apertures link each chamber to the external medium, an anterior nostril through which water enters the chamber and a posterior nostril through which water leaves (figure 2). The anterior nostril may be an open hole, a tube or, in one exceptional case – the ribbon moray, *Rhinomuraena quaesita* – a funnel. The posterior nostril may be an open hole, a slit or a tube. Unlike the noses of air-breathing vertebrates, which are connected to the mouth and perform both olfactory and respiratory functions, the olfactory organs of fish are usually isolated from the mouth and perform only their eponymous function.

There are many exceptions to this general pattern. For example, lampreys and hagfish possess only a single olfactory organ and a single nostril (*e.g.* Kleerekoper & van Erkel 1960; Theisen 1973), and in hagfish the olfactory organ is not isolated from the mouth. In many flatfish the two olfactory organs are located asymmetrically on the head (Norman 1934, p. 14). In the European plaice, *Pleuronectes platessa*, for instance, one organ (the "eyed-side" organ) lies between and just in front of the eyes, on the dorsal surface of the fish; the other ("blind-side") organ lies laterally to its left eye. The sensory region in needlefish, halfbeaks and flying fish is situated in a

shallow triangular pit rather than a chamber (*e.g.* the garpike, *Belone belone* [Theisen *et al.* 1980]) (figure 3). The olfactory organs in various sharks are located on the ventral surface of the snout (Theisen *et al.* 1986; Zeiske *et al.* 1987). The olfactory organs in puffers protrude from the dorsal surface of the fish on stalks (figure 4; see also video clip described in Appendix A.1): in the puffer *Takifugu pardalis* (Wiedersheim 1887) and the Northern puffer, *Sphoeroides maculatus* (Copeland 1912), the sensory region is located within a chamber mounted on a stalk; in the blackspotted puffer, *Arothron nigropunctatu*s (Wiedersheim 1887), the olfactory organ is split into two unequal, fairly rigid flaps. The sensory region is located on the inside of these flaps, and exposed to the environment. In short, the olfactory organs of fish display considerable variety.

The sensory region (*i.e.* olfactory epithelium – the two terms are used interchangeably here) may be located either on the floor and sides of the olfactory chamber (*e.g.* the striped panchax, *Aplocheilus lineatus* [Zeiske 1974]), or on an irregularly-shaped boss (*e.g.* the garpike [figure 3]), or, more typically, on thin flexible folds (Kleerekoper 1969, pp. 42-51). These folds, or lamellae, also arise from the floor of the olfactory chamber and may be supported by attachment to the side of the chamber. Each lamella comprises two layers of epithelium and an intervening layer of connective tissue. The olfactory epithelium is found on both sides of a lamella, coating all or part of it. The lamellae of some fish have secondary folds, and occasionally (Chen & Arratia 1994, figure 4*d*) tertiary folds. Secondary folds may (*e.g.* Theisen *et al.* 1986, p. 77) or may not (Yamamoto & Ueda 1977, p. 1164) be coated with olfactory epithelium.

The number of lamellae present in the olfactory chamber varies from one to about 300, depending on the species and the age of the fish. Multiple lamellae adopt several arrangements (Holl 1965, figure 48), again depending on the species. Arrangements pertinent to this article are shown in figure 5. In one, referred to here as the longitudinal array (figure 5*a*), the lamellae lie parallel to the axis between the anterior and posterior nostril. In another (figure 5*b*), the lamellae branch from a fold or ridge (the raphe) that runs along the axis between the anterior and posterior nostril to create a rosette-like structure (and referred to here as a rosette). In eels and catfish the olfactory rosette may contain large numbers of lamellae (up to 291 in the catfish

Pseudoplatystoma corruscans, according to a figure cited in Schulte & Riehl 1978, p. 127), and as a result appears elongated (figure 5*c*)[1]. In some cases the lamellae are arranged around a central axis in a radial fashion (*e.g.* sturgeon: Chen & Arratia 1994, figure 5). One of the most sophisticated lamellar systems, however, occurs in the olfactory organ of the family Polypteridae (bichirs), and essentially consists of six elongated rosettes fused together in a radial fashion to form an extremely compact unit (Pfeiffer 1968; Theisen 1970; see also Zeiske *et al.* 1992, figure 2.5).

Longitudinal arrays of olfactory lamellae and elongated olfactory rosettes are notable for their uniformly spaced, parallel lamellae (figures 5*a* and 5*c*; see also Ngai *et al.* 1993, figure 1*d*). One advantage of this arrangement, where the olfactory epithelium is effectively deployed on a set of parallel plates, compared to one consisting of a set of circular pipes, for example, is that fully developed (*i.e.* parabolic) flow is, on the average, closer to the lamellar surface, and therefore the distance over which an odorant must travel to reach the olfactory epithelium is less (figure 6). It should also be noted that even olfactory chambers that lack well-defined lamellae, such as those of the striped panchax (Zeiske 1974), and the round goby, *Neogobius melanostomus* (Belanger *et al.* 2003), could be regarded as a single pair of parallel plates, albeit a convoluted one (see, for example, Zeiske 1974, figure 3*c*). In addition, for a given cross-sectional area, a parallel plate-like channel will expose more wetted surface to the fluid than a circular pipe, leading to more efficient odorant capture (the rate at which a species is adsorbed at a surface is proportional to the area of that surface [Schmidt-Nielsen 1997, p. 586]).

Although it has been shown that fish with olfactory lamellar arrays are particularly sensitive to certain compounds (*e.g.* the European eel [Teichmann 1959, p. 244], striped eel catfish [Theisen *et al.* 1991, p. 133] and goldfish [Bjerselius & Olsén 1993, p. 432]), fish lacking olfactory lamellar arrays (*e.g.* the round goby) may also be sensitive to certain compounds (Murphy *et al.* 2001, figure 6). Thus whilst a well-developed olfactory organ undoubtedly contributes to olfactory acuity, other factors, such as the structure and cellular composition of the olfactory organ (Yamamoto 1982; Hamdani *et al.* 2006), will also play important parts.

[1] The figure usually cited for the largest number of olfactory lamellae in an elongated rosette is 230, for the olfactory organ of the Mexican barred snapper, *Hoplopagrus guentherii* (Pfeiffer 1964, Table I).

3. BOUNDARY LAYERS

The relative movement of a fish in water will generate a boundary layer on its surface (for general discussions of boundary layers see Massey 1989, pp. 148-150 and Chapter 8; Vogel 1994, Chapter 8). Boundary layers will act as barriers to transport of odorant molecules to the sensory surface: the thicker the boundary layer, the greater the barrier it provides (Vogel 1994, pp. 161-162). Denny (1993, pp. 138-140) pointed out that the presence of a boundary layer will result in a delay in the fish detecting an odorant in its immediate surroundings. He also pointed out that this problem would be alleviated by having the anterior nostril as far forward as possible on the head (where the boundary layer will be thinnest), by raising the entrance to the olfactory chamber above the surface of the head (thus projecting it into or through the boundary layer), by swimming fast (reducing the thickness of the boundary layer), and by actively drawing fluid into the olfactory chamber.

Typically the anterior nostrils of fish do indeed tend to be situated towards the tip of the snout (figure 7). The tubular anterior nostrils of some fish are also level with, and may even protrude beyond, the snout. For example, the tubular anterior nostrils of the European eel, *Anguilla anguilla*, are at least level with the tip of the snout (personal observation, preserved specimen). Bateson (1890, p. 230) describes the tubular anterior nostrils of the European conger, *Conger conger*, as "projecting beyond the surface of the nose". The funnel-like anterior nostrils of the ribbon moray clearly extend beyond the tip of the snout (Holl *et al.* 1970, figure 1), as do the tubular anterior nostrils of the bichir *Polypterus endlicheri* (personal observation). In addition to minimising the effect of the boundary layer, according to Stoddart (1980, p. 26) laterally protruding tubular nostrils also help locate the source of an odour.

Denny (1993, figure 7.20) illustrated how many fish do in fact have anterior nostrils that are raised slightly above the surface of the head of a fish. This feature can also be seen clearly in Burne's (1909, p. 614) picture of the olfactory organ of the haddock, *Melanogrammus aeglefinus*. Burne (1909, p. 613) even describes the anterior rim of the anterior nostril of this organ as a "low tubular lip". A crude calculation suggests that the boundary layer for a haddock would be about 1 mm thick at the anterior nostril (Appendix A.2). (This figure is in agreement with actual measurements

recorded from a swimming fish – *e.g.* Anderson *et al.* 2001, figure 5*a*.) The anterior rim of the anterior nostril of this specimen is raised about 0.1 mm above the surface. Even this small distance would be sufficient to reduce the lag time, however (Denny 1993, figure 7.19).

In some fish, including puffers, the olfactory organ *itself* is elevated above the surface of the fish (Section 2). (Wiedersheim [1887] suggested that the olfactory organs in puffers have been displaced onto the surface of the fish by the excessive development of the jaw muscles, the latter enabling the fish to cut through shell and coral.) Copeland [1912, p. 363] states that the olfactory organ of the Northern puffer is raised 4 mm above the dorsal surface of the snout (length of fish not given), which is certainly in accord with an estimate (5 mm) made on the olfactory organs of a live specimen of a blackspotted puffer (figure 4). Another crude calculation suggests that the boundary layer of a blackspotted puffer is about 2 mm thick in the vicinity of the olfactory organs (Appendix A.2), in turn suggesting that the olfactory organs will protrude through this layer. Whilst making these observations, it was noticed that the olfactory flaps of the puffer occasionally trembled, a movement that the puffer itself seemed to cause and be in control of (as opposed to one arising from an external current) (see Appendix A.1 for details of a video clip demonstrating this trembling behaviour).

With regard to fish swimming fast in order to reduce the thickness of the boundary layer, it is interesting to note that blind cave fish, *Astyanax jordani*, tend to swim faster on encountering a new environment (Teyke 1985). Whilst this behaviour might be attributed to the stimulation of the mechanosensors of the fish's lateral line system, there might also be an olfactory component to it, especially in light of the fact that the lateral line and olfactory systems of the related blind Mexican cave fish (*Astyanax fasciatus*) are linked (Baker & Montgomery 1999, p. 526).

The effect of the boundary layer will also be offset when water is actively drawn into the olfactory chamber, either via the beating of cilia or through the pumping action of accessory sacs. These two mechanisms are discussed in Section 4.

4. VENTILATION MECHANISMS

Diffusion times are long even over comparatively short distances in water: an odorant-like molecule will take (using equation A.3, Appendix A.3) just under 10 minutes to diffuse 1 mm in water. Thus a fish must actively draw water into its olfactory chamber in order to receive an olfactory stimulus in good time. Furthermore, the sizes of the olfactory organs of fish are typically on the order of millimetres, and are not usually more than a centimetre or so. For example, in a large specimen of a longnose gar, *Lepisosteus osseus* (1.5 m total length), the size of the olfactory organ is just under 1 cm. Therefore water must also be actively circulated *around* the olfactory chamber. Although diffusion times (again calculated using equation A.3) in the olfactory lumen[2] (depth typically 10 – 70 μm [Appendices A.4, A.6.1 and A.6.2]) are much shorter (0.01 – 0.6 s), one can show that here too transport to the olfactory epithelium is dominated by convection (the bulk movement of fluid [Denny 1993, p. 91; Bejan 1993, pp. 216-218]), *i.e.* by water being actively circulated through the olfactory lumen (Section 7). A flow of water within the olfactory lumen will help maintain the concentration gradient of odorant between the aqueous phase and the sensory surface, favouring the final step in the transport process (LaBarbera & Vogel 1982, p. 56), a step that will involve diffusion alone (Vogel 1994, pp. 196-197).

Water may be actively drawn into, circulated within, and indeed expelled from, the olfactory chamber by at least three means. The first is the beating of the cilia of non-sensory cells ("kinociliated" cells), which may be found both on the olfactory lamellae (*e.g.* Yamamoto & Ueda 1978a, figure 10) and other surfaces throughout the chamber (*e.g.* the walls: Døving *et al.* 1977, p. 248 and their figure 4*a*). Each kinociliated cell bears many such cilia; some kinociliated cells may have up to 160 (Schulte & Holl 1971, p. 261). The cilia themselves are generally 10 – 20 μm long (*e.g.* Cancalon 1978, p. 388; Hansen *et al.* 1999, p. 329), indicative of the fact that they propel water – cilia that propel mucus are shorter (Sleigh 1978, p. 257 and p. 264; 1989, p. 363). One exception is the cilia on the olfactory lamellae of zebrafish (*Danio rerio*), which were reported to be shorter (7-8 μm) (Hansen & Zeiske 1998, p.

[2] The olfactory lumen is here defined as the channel in which the olfactory epithelium is located. This may be the olfactory chamber itself (*e.g.* in the case of the striped panchax) or it may be the channel between two adjacent lamellae (*e.g.* in the case of the elongated olfactory rosette of an eel).

46), suggesting that they propel mucus and not water. Water currents generated by the beating olfactory cilia of fish have in fact been observed indirectly *in vivo* and *in vitro* using dye and particles (Teichmann 1959, pp. 240-243; Bashor *et al.* 1974, p. 778; Døving *et al.* 1977, p. 249).

In some cases, as Teichmann (1959, p. 240) demonstrated by visualising the flow (with particles of ground charcoal) into and around the olfactory chamber of an anaesthetised (*i.e.* stationary) eel, the beating of cilia *alone* is sufficient both to draw water into the chamber and to circulate water within it. However in other cases it is not sufficient to draw water into the chamber (*e.g.* sharks, Section 9).

Beating cilia generate steep velocity gradients adjacent to the surface over which they are driving the flow (Jahn & Votta 1972, figure 12; Nielsen *et al.* 1993, figures 7 and 12; Vogel 1994, p. 349). Steep velocity gradients augment the rate of transfer (*e.g.* of odorant) to a surface (Vogel 1994, pp. 196-197 and pp. 355-356). Thus if present in the olfactory epithelium, as they are for example in the European eel (Holl 1965, figure 15), and other eels (Yamamoto & Ueda 1978b, p. 1208), odorant transport should be augmented. Bashor *et al.* (1974, p. 779) noted that the beating action of cilia was likely to favour efficient odorant transport to the olfactory epithelium in their study of flow in the olfactory chamber of the longnose gar.

It should be noted that in many species of fish kinociliated cells are absent from the olfactory chamber (*e.g.* Table 1).

The second means for actively ventilating the olfactory chamber is through the pumping action, effected by their expansion and compression, of accessory sacs. Accessory sacs may be direct expansions of the main olfactory chamber (*e.g.* in the striped eel catfish, *Plotosus lineatus* [Theisen et al. 1991]) or may be separate chambers connected to the olfactory chamber by short ducts (*e.g.* in the striped panchax [Zeiske 1974]) (figure 8). Data on the capacity of accessory sacs, expanded or compressed, are scant; where measurements have been made, they suggest that their volumes vary from a few mm^3 to a few hundred mm^3 (*e.g.* Eaton 1956, p. 199; Kleerekoper & van Erkel, 1960, p. 220; Holl & Meinel 1968, p. 410). Expansion of an accessory sac can cause water to be drawn into the olfactory chamber and its

contraction can cause water to be expelled. A valve, if present, ensures that water flows through the chamber in a unidirectional fashion. The valve is usually situated on the posterior nostril in the form of one or two thin lips (Burne 1909).

Expansion or contraction of the accessory sac may be involuntary or voluntary. The involuntary action is a by-product of the respiratory process (*e.g.* Liermann 1933, p. 21). Normally as a fish breathes it opens and closes its mouth. Opening its mouth causes the sac to expand; closing its mouth causes the sac to contract. The actual mechanism for expansion/contraction may be mechanical, through the movements of bones and muscles in the upper and lower jaws (*e.g.* Burne 1909, p. 641) and, in some cases, through the movement of the gill cover (*e.g.* Liermann 1933, pp. 13-14), or hydraulic, as a result of pressure changes in the mouth arising during respiration (*e.g.* Melinkat & Zeiske 1979). Because the respiratory movements are rhythmic, the flow of water through the olfactory chamber as a result of the expansion and contraction of the accessory sacs is also rhythmic (*e.g.* Liermann 1933, p. 21) (although see Section 8).

Voluntary expansion and contraction of the accessory sacs may occur as the result of spontaneous and rapid jaw protrusion ("coughing") in the case of certain flatfish (Nevitt 1991), or snapping of the jaws in the case of skipjack tuna, *Katsuwonus pelamis* (Gooding 1963, p. 1630), or from movement of the maxillary barbel in some catfish (Burne 1909, pp. 624-626; Alexander 1965, p. 108). These voluntary actions, which permit the fish to deliberately sample the surrounding environment, have been likened to sniffing (Burne 1909, p. 625 and p. 662; Gooding 1963, p. 1630; Nevitt 1991). Certainly Nevitt (1991, p. 13) was able to show that the coughing behaviour in the flatfish she studied had an olfactory component to it.

As for kinociliated cells, many species of fish do not have accessory sacs (*e.g.* Table 1). If they are present, they usually occur singly, or as an asymmetric pair. Note that the presence of an accessory sac may give the fish the ability to sniff.

In rare cases the olfactory chamber may be ventilated by the respiratory flow. For example, in hagfish the respiratory flow enters the single nostril, passes along the nasal duct and then through the olfactory chamber on its way to the gills (Strahan

1958, p. 227). Flow is maintained by the rhythmic furling and unfurling of a flap of tissue (the velum) lying posterior to the mouth (Strahan 1958), in addition to muscular contractions (Johansen & Hol 1960, p. 478); flow is therefore also rhythmic (Strahan 1958, p. 229).

Circulation of water within the olfactory chamber of a fish might also be assisted by mechanical agitation of the chamber. This could occur if part of an accessory sac were located beneath the olfactory chamber, as it is, for example, in the snakeheads *Channa marulius* and *punctata* (Burne 1909, pp. 636-637; Kapoor & Ojha 1973, p. 99). Curiously, Zeiske *et al.* (1976, pp. 262-263) suggest that the microridge surface patterns on the non-sensory epithelium of the olfactory chamber of the striped panchax and the green swordtail, *Xiphophorus hellerii*, may be present to cope with strain caused by the movement of the single accessory sac of these fish, which also partly resides beneath the olfactory chamber (*e.g.* figure 8). Zeiske (1973, p. 15) alludes to possible mobility in the olfactory chambers of these types of fish elsewhere.

The pressure changes caused by the pumping action accessory sac may also cause mechanical agitation of the olfactory chamber: Nevitt (1991, p. 6) noticed that the nostrils of the eyed-side olfactory organ of a rock sole, *Lepidopsetta bilineata*, were drawn together slightly during normal respiration and Theisen (1982, p. 252) observed the lateral wall of the olfactory chamber of the sea stickleback, *Spinachia spinachia*, bending inwards and outwards during normal respiration, as did Solger (1894) in the three-spined stickleback, *Gasterosteus aculeatus*.

Finally, mechanical agitation of the olfactory chamber may also result from the movement of jaw bones during respiration. For instance, inspection of the skull of the catfish *Sisor rabdophorus* suggested to Ojha and Kapoor (1974, p. 129) that the olfactory chamber would be agitated by the palatine bone as the fish breathes. Liermann (1933, pp. 13-14) also deduced that the lachrymal bone of the European perch, *Perca fluviatilis*, depresses the roof of the olfactory chamber in a rhythmic fashion during the course of normal respiration.

In assisting circulation of water within the olfactory chamber, mechanical agitation should lead to a more uniform concentration of odorant within the olfactory chamber,

in turn leading to a very steep concentration gradient between the fluid within the chamber and the olfactory epithelium and an improved net flux of odorant molecules to the olfactory epithelium (LaBarbera & Vogel 1982, p. 56).

It is often stated that, in some cases at least, a current of water through the olfactory chamber may be generated by the forward motion of the fish (*e.g.* Burne 1909, p. 661). A more precise way of stating this would be to say that any *relative* motion of water with respect to the fish (in an anterior to posterior direction) will generate a current through the chamber. Thus a current could still be generated if the fish was stationary but facing an oncoming current. Or flow through the olfactory chamber could be enhanced if the fish were swimming into an oncoming current. The various ways in which flow through the olfactory chamber may be generated from an external flow are explored in detail in the next section.

5. HARNESSING EXTERNAL FLOWS

Several authors have suggested, and shown, that animals use external flows to generate a secondary flow through some part of their bodies, or some structure that they build (Sattler & Kracht 1963; Wallace & Sherberger 1975; Vogel 1994, p. 60 and pp. 70-73, and references therein).

There are three main mechanisms that give rise to these secondary flows (Vogel & Bretz 1972; Vogel 1977a; Vogel 1978; Vogel 1994, p. 60 and pp. 70-73). One of these occurs when one opening of an L-shaped tube is directed into an oncoming flow (Vogel 1978, p. 108). This opening will experience almost the total pressure of the flow (static plus dynamic), whilst the opening perpendicular to the flow will experience only the static pressure of the flow. The resultant pressure difference will drive a secondary flow from the opening directed into the flow to the opening perpendicular to the flow. Pitot tubes that are used to measure velocity of flow in a fluid operate using this mechanism (Massey 1989, pp. 98-101; Vogel 1994, pp. 58-60), which is consequently referred to here as the Pitot-like mechanism.

In another mechanism, the pressure difference driving the secondary flow is caused by a difference in velocity at the two openings of a chamber, resulting either from one opening being elevated with respect to another in a boundary layer, or a difference in free-stream velocities at the two openings (Vogel & Bretz 1972; Vogel 1994, pp. 70-73). Venturi meters, which, like Pitot tubes, can also be used to measure velocity of flow, operate on the basis of this mechanism (Massey 1989, pp. 101-103; Vogel 1994, pp. 57-58), which is consequently referred to here as the Venturi-like mechanism. In contrast to the Pitot-like mechanism, the Venturi-like mechanism does not depend on the direction of the flow (Vogel & Bretz 1972, p. 210); however, the pressure difference is not as great as that generated by the Pitot-like mechanism (Vogel *et al.* 1973, p. 11).

A swimming fish would also have to expend energy in overcoming the (probably) small amount of drag associated with the secondary flow.

The final mechanism considered here for causing a secondary flow is viscous entrainment. This occurs when a fluid passing over an opening of a tube perpendicular to a current draws fluid out of that tube (Vogel 1994, p. 72). The phenomenon arises because the slow moving or stationary fluid just beneath the opening is subject to a large shear force by the fluid moving rapidly over the opening. In resisting this force, the stationary or slow moving fluid is drawn out of the tube. The larger the hole (or the faster the flow over it), the greater the entrainment (Vogel 1978, p. 108) and, unless the hole is infinitesimal, the fluid in the hole will always be set in motion by the fluid passing over it (Shaw 1960, p. 550). Viscous entrainment may operate in conjunction with either a Pitot- or Venturi-like mechanism, and indeed it is difficult to separate it from either (Vogel 1974, p. 445).

Do any of these mechanisms operate in fish? There are four reasons that suggest the Pitot-like mechanism might. First, the pressure coefficient on the surface of a swimming fish between the tip of the snout and the eye is positive (Dubois *et al.* 1974, figures 4 and 5; Vogel 1994, pp. 67-68). Second, it has long been recognised that some fish possess adaptations – depressions in front of the anterior nostril, funnels, hoods, external and internal flaps (*e.g.* figure 2) – to direct flow into the olfactory chamber (Burne 1909, p. 661; Kleerekoper 1969, p. 60; Theisen *et al*. 1986,

p. 74; Zeiske *et al*. 1987, p. 2411; Zeiske *et al*. 1994). Third, some of these adaptations, notably the funnels, hoods, and external flaps, are likely to halt flow locally (*i.e*. at the entrance to the anterior nostril) (Vogel 1994, pp. 81-82; Massey 1989, p. 98), augmenting the pressure difference between the anterior and posterior nostrils. Fourth, in fish with these adaptations, the anterior and posterior nostrils are arranged roughly at right angles to each other, with the opening of the anterior nostril directed forwards, into the oncoming flow, and the posterior nostril directed upwards, downwards or to the side of the fish, and therefore roughly perpendicular to the oncoming flow.

One specific example of a fish in which a Pitot-like mechanism is likely to operate is a marine species of catfish, the hardhead sea catfish, *Ariopsis felis* (Zeiske *et al.* 1994). The olfactory organs of this fish are situated close to the edge of the snout [the anterior nostril is about 3 mm away from the edge of the snout in the 18 cm specimen shown in figure 1 of Zeiske *et al.* (1994)], where the pressure coefficient on the surface of the fish will be close to its maximum. In addition, the olfactory organ has a forward-pointing, funnel-shaped anterior nostril set at right angles to the posterior nostril (Zeiske *et al*. 1994, figure 2). Furthermore, it "is an almost permanent swimmer" (Zeiske *et al.* 1994, p. 120). The pressure difference across the olfactory chamber of the hardhead sea catfish arising from the Pitot-like mechanism may be estimated to be 21 – 46 Pa (Appendix A.5).

Other examples of fish in which a Pitot-like mechanism is likely to operate are given in Table 1.

The possibility that a Pitot-like mechanism might ventilate the olfactory organs of some fish has been alluded to before. Zeiske *et al*. (1994, p. 120) remark that a pressure difference between the anterior and posterior nostrils of the hardhead sea catfish will provoke a flow; Theisen *et al*. (1986, p. 81) and Zeiske *et al*. (1987, p. 2410) make similar comments for sharks. Settles (2005, p. 201) also mentions that flow from the posterior nostril of a fish "vents to local static pressure", and refers to "a fluted Pitot-tube-like anterior naris [nostril] extension" in the bichir, *Polypterus bichir* (Waldschmidt 1887, figure 1).

The possibility of a Venturi-like mechanism to drive flow through the olfactory organ of a fish has also been raised before, by Vogel (1977a, p. 294; 1978, p. 113), although no specific examples were given. Since fish may orient themselves to an external current, and therefore harness the greater pressure differences generated by a Pitot-like mechanism for induced flow, one would have thought that ventilation of the olfactory organ of a fish by a Venturi-like mechanism would be a rare occurrence. The olfactory organ of the Northern pike, *Esox lucius*, might be a possible candidate for a Venturi-like mechanism, however (inset, figure 1). The anterior nostril of the olfactory organ of this fish, which notably lacks an external flap or hood to guide flow into it (figure 2), is roughly flush with the surface of the head (Burne 1909, p. 628), rather than directed forwards, and the posterior nostril is raised with respect to its anterior counterpart, as required for a Venturi-like mechanism. The anterior nostril is wide and has a low, well-rounded edge, whilst the crescent-shaped posterior nostril is sharp-edged (sharp-edged exits minimise energy losses due to friction [Massey 1989, p. 92]), highly reminiscent of the openings of prairie dog burrows, which are also likely to be ventilated by a Venturi-like mechanism (Vogel *et al.* 1973). The pike is a rather sedentary fish (Wheeler 1969, p. 166), so that the direction of flow over its nostrils could vary, in which case a Venturi-like mechanism would be advantageous.

The olfactory organ of the sterlet, *Acipenser ruthenus*, which unlike the pike swims continuously (personal observation), also has a narial arrangement suggestive of a Venturi-like mechanism. Here, though, the posterior nostril is much wider than that of the pike, and lies more laterally on the surface of the head (figure 9). The wider posterior nostril is probably due to the fact that the sterlet is an active swimmer (personal observation), and would therefore benefit more from viscous entrainment (below) than the pike. The posterior nostril also protrudes noticeably from the surface of the fish, presumably to enhance the pressure difference across the olfactory chamber, and therefore the induced flow through it, again in a similar manner to a prairie dog burrow (Vogel *et al.* 1973, p. 11).

Flow through any olfactory organ in which the posterior nostril is an open hole (*e.g.* the hardhead sea catfish, the Northern pike, or the sterlet) is likely to profit significantly from viscous entrainment; even where the posterior nostril is a slit, as in

the reedfish, *Erpetoichthys calabaricus* (Theisen 1970, figure 1), flow through the organ might be assisted by viscous entrainment.

6. REYNOLDS NUMBER IN THE OLFACTORY LUMEN

The Reynolds number of a fluid dynamic system is a ratio of inertial forces to viscous forces (Massey 1989, pp. 134-141; Vogel 1994, pp. 86-88). Knowing the Reynolds number for flow over the olfactory epithelium of a fish is important because it indicates the nature of the flow - laminar or turbulent (Vogel 1994, pp. 84-85). At high Reynolds numbers (>2,000 for a long, straight, cylindrical tube [Vogel 1994, p. 85]), inertial forces predominate, favouring turbulence; at low Reynolds numbers, viscous forces predominate, favouring laminar flow (Vogel 1994, p. 87). The nature of the flow will in turn determine the rate of transfer of odorant from the aqueous phase to the olfactory epithelium: transfer in a turbulent regime is faster (Vogel 1994, p. 161), although frictional losses will be greater. Reynolds numbers (*Re*) may be calculated using the equation:

$$Re = \frac{lu}{\upsilon} \tag{6.1}$$

where l is the characteristic length of the system, u is the velocity of flow, and υ is the kinematic viscosity of the fluid (Vogel 1994, p. 85). Here the characteristic length of the olfactory lumen is taken to be its depth (figure 5*c*).

In order to estimate the Reynolds number of the flow over the olfactory epithelium of a fish one therefore needs to know the depth of the olfactory lumen and the velocity of flow in this channel. Whilst data on the depth of the olfactory lumen of various fish is readily available, there is no data on the velocity of flow in the olfactory lumen. In the two estimates made here the velocity in the lumen was inferred from other sources, a situation which clearly is not ideal.

The first estimate of Reynolds number is for flow within the olfactory lumen of the striped panchax and green swordtail (Appendices A.6.1 and A.6.2). In these fish, the

olfactory chamber is ventilated primarily through the pumping action of a single accessory sac (Zeiske 1973, 1974) (figure 8) - kinociliated non-sensory cells are absent from the chamber (Zeiske 1973, p. 6; Zeiske *et al*. 1976)[3]. Peak velocities of flow at the entrance to the anterior nostril of these chambers have been measured by laser Doppler velocimetry (Kux *et al*. 1978). From the anatomical data of Zeiske (1973, 1974) and Kux *et al.* (1978, 1988), one can estimate the cross-sectional areas of both the anterior nostril and the olfactory lumen, and then use the principle of continuity (Vogel 1994, pp. 32-34) to estimate the average velocity of flow in the olfactory lumen. Together with figures for the depth of the olfactory lumen from Zeiske (1974), the Reynolds number for flow in the olfactory lumen of the striped panchax at 25 °C may be estimated to be 0.3 – 4 (Table 2). A similar range of Reynolds numbers (0.09 – 0.9) may be obtained for the green swordtail from the data of Kux *et al.* (1978, 1988) and Zeiske (1973) (Table 2); the latter range is likely to be an underestimate, however (Appendix A.6.2).

These estimates assume that the olfactory chambers of the striped panchax and green swordtail are static, which they may not be, particularly given that part of the accessory sac is located beneath the floor of the olfactory chamber (*e.g.* figure 8; see also Section 4).

The estimated average velocities in the olfactory chamber of the striped panchax and green swordtail (Table 2) are an order of magnitude greater than those measured in the interior of a model of the olfactory chamber of the green swordtail (Kux *et al.* 1988). This discrepancy may be due to the fact that the model, which was 200 times larger than the actual olfactory chamber, also reproduced (a static version of) the accessory sac at the back of the chamber; flow through the model chamber subsequently passed through this feature, an arrangement that may have had an adverse effect on the flow.

The second estimate of the Reynolds number is for flow over the olfactory epithelium of the channel catfish, *Ictalurus punctatus*. The olfactory epithelium of the channel

[3] Later papers (Melinkat & Zeiske 1979, p. 355; Kux *et al.* 1988, p. 258) refer to Zeiske *et al.* 1976 in stating that kinociliated cells are absent from the olfactory chamber of the striped panchax. However, Zeiske *et al.* (1976) do not state explicitly that these cells are absent.

catfish is located on lamellae arranged in an elongated rosette (Caprio & Raderman-Little 1978). The olfactory epithelium coats only part of each lamella; the greater part is coated with kinociliated cells (figure 10). Given that the length of the cilia on these cells is 15-20 μm (Cancalon 1978, p. 388), it may be assumed that they propel water rather than mucus (Section 4). One may also assume, then, that flow over the olfactory epithelium is achieved primarily by the beating of cilia (the olfactory organ of the channel catfish lacks accessory sacs). Although there are no *in vivo* data for the velocity of flow within the interlamellar space of the olfactory organ of the channel catfish, the velocity of water currents generated by beating cilia has been measured in other studies. Thus Bashor *et al.* (1974, p. 778) found that the velocity of a dye front moving across the surface of an excised lamella from the olfactory chamber of the longnose gar generated by the beating of cilia was between 1.5 and 2.9 mm s^{-1}, with an average of 2.2 mm s^{-1} (admittedly the olfactory lamellae of this fish have secondary lamellae). While one must be careful interpreting hydrodynamic data obtained from dye studies (Lim 2000, p. 44), and especially in this case where the lamella was isolated, this average agrees remarkably well with the figure of 1.7 mm s^{-1} obtained for the mean velocity of flow in the 40 μm deep gill of the blue mussel, *Mytilus edulis*, which is also lined with kinociliated cells (Nielsen *et al*. 1993, p. 61 & 70). The depth of the olfactory lumen of the channel fish can be estimated from various micrographs to be 10 – 70 μm (Appendix A.4). A velocity of 2 mm s^{-1} in a channel this deep would give a Reynolds number in the range 0.02 - 0.2 at 25 °C.

Thus all the above estimates indicate that flow within the olfactory lumen is laminar (Reynolds number lying between about 0.02 and 4).

There are two previous estimates of the Reynolds number within the olfactory chamber of a fish. The first was made by Atema (1988), who, again using a figure for the maximum velocity of flow at the anterior nostril obtained by laser Doppler velocimetry (Kux *et al.* 1977; not Kux et al. 1978 as stated by Atema) and the principle of continuity, suggested that the Reynolds number for flow in the olfactory lumen of the striped panchax/green swordtail was about 1. (Although Atema does not state this figure explicitly, one may infer it from the previous discussion in the same text on copepod feeding currents [Atema 1988, p. 42]). However, whilst Atema's

estimate certainly agrees with the ones shown in Table 2, it is not entirely clear how he arrives at the average velocity in the chamber from the "gross morphological measurements" he mentions.

The second previous estimate of Reynolds number within the olfactory chamber of a fish was made by Nevitt (1991, p. 15). She used nasal casts to estimate the volume change in the eyed-side olfactory organ (comprising an olfactory chamber and two accessory sacs) during a "coughing" event in starry flounders, *Platichthys stellatus*. From the time taken for the coughing event it is possible to calculate the flow rate through the organ, and from an estimate of the cross-sectional area of the olfactory chamber to determine the average velocity through the chamber. From this figure the Reynolds number may be estimated to be about 300 – 600 (Appendix A.6.4). Clearly the numbers in this range are much greater than the values shown in Table 2. However, it must be remembered that this range refers to flow through the *entire* chamber, and not specifically to flow over the olfactory epithelium. (One assumes that the olfactory epithelium of the starry flounder, since it belongs to the subfamily Pleuronectinae, is deployed on lamellae in a longitudinal array. All members of this subfamily, apart from two *Atheresthes* species, have a longitudinal olfactory array [Norman 1934, p. 41].) It is not known whether the olfactory lamellae of the starry flounder possess kinociliated cells.

7. PÉCLET NUMBER IN THE OLFACTORY LUMEN

The relative contributions of convection and diffusion to the rate at which odorant is transported from the olfactory lumen to the surface of the olfactory epithelium can be gauged using the Péclet number (*Pé*):

$$Pé = \frac{lu}{D} \qquad (7.1)$$

where l is taken to be the lumen depth (as for the Reynolds number, Section 6), u here is the average velocity of the fluid in the lumen and D is the diffusion coefficient of

the odorant in water (Denny 1993, pp. 91-92; Vogel 1994, pp. 313-314; Vogel 2004). A Péclet number greater than 1 would suggest that transport of the odorant to the olfactory epithelium is dominated by convection, a number less than 1 that transport is dominated by diffusion and a number equal to 1 that the two processes are balanced.

The Péclet numbers for flow over the olfactory epithelia of the striped panchax, green swordtail and channel catfish (*i.e.* the same fish which feature in Section 6) are shown in Table 2. The values are greater than 1, indicating that transport of the odorant to the olfactory epithelium is controlled by convection, which in one respect is not surprising, since the olfactory lumina of these fish are actively ventilated either by the pumping action of an accessory sac or the beating of cilia (Section 6).

However, one might expect that the processes of diffusion and convection would be balanced in a well designed biological system (here the olfactory lumen) (Vogel 2004, p. 392). That they are not in the above cases suggests that these pumping mechanisms are not metabolically costly to the fish. One could in fact estimate the power (P) required to pump water through the olfactory chamber using the equation $P = Q\Delta p$ (Vogel 1994, p. 324), where Q here would be the flow rate through the chamber and Δp the pressure difference across it. Unfortunately there is only one case, that of the starry flounder, in which Δp has been measured across the olfactory chamber of a fish (Nevitt 1991). From these measurements the power required to pump water through the olfactory chamber during either normal respiration or a coughing event (Section 6) may be estimated (Appendix A.7); it is only a small fraction of the resting metabolic rate of a flounder (≤ 0.1 %), and is certainly not as much as required to pump water across the gills, an activity thought to cost at least 4 – 6 % (Steffensen & Lomholt 1983) and possibly as much as 15 % (Cameron & Cech 1970, p. 453) of the resting metabolic rate of a fish.

8. VORTICES

A vortex (Lugt 1983, pp. 18-19; Vogel 1994, pp. 204-212) in or around the olfactory organ could benefit the olfactory process in two ways. First, it could enhance the transfer (Vogel 1994, p. 212) of odorant to the sensory surface. Second, it could

entrain fluid through the olfactory chamber, thereby assisting ventilation of the olfactory chamber (Balsam & Vogel 1973, p. 981; Vogel 1978, p. 114).

Vortices, which may form at solid-fluid interfaces "provided Reynolds numbers are decently above unity", can be generated by several different mechanisms (Vogel 1994, pp. 212-218). Three in particular seem relevant to olfaction in fish.

In the first, a vortex is generated when fluid moves rapidly over an opening or pit; this vortex may generate a secondary vortex further within these features provided they are narrow and deep (Vogel 1994, p. 213). This mechanism might operate when water that is being expelled from an accessory sac through the posterior nostril passes the olfactory chamber (figure 11). The expelled water could give rise to a vortex at the back of the chamber (if the accessory sac is located at the back of the chamber, as most are) resulting in enhanced odorant transfer and possible entrainment of water through the anterior nostril. If water is entrained through the anterior nostril by this putative vortex, the result would be an almost continuous (and unidirectional) flow of water through the chamber (even in the absence of a vortex there is likely to be some entrainment – Section 5). The Reynolds number for flow in the accessory sac duct at the back of the olfactory chamber of the striped panchax lies between 3 and 10 (Appendix A.6.5), and so a vortex here is not out of the question.

A vortex might similarly be generated in the olfactory pit of the garpike (Section 2) (figure 3). Adult garpike lack kinociliated cells (Theisen *et al.* 1980, p. 167) and must therefore rely on other means to ventilate the olfactory epithelium. They are known to "swim continuously and normally rather fast" (Theisen *et al.* 1980, p. 169) and so the movement of water over the surface of the pit might create a vortex and thus the necessary ventilation. The Reynolds number for flow directly above the olfactory pit of a swimming garpike is about 5,000 (Appendix A.6.6), suggesting that conditions are certainly favourable for vortex formation. There are several interesting features of the garpike olfactory pit which probably also have a bearing on its hydrodynamics. Specifically, some of the edges of the pit form sharp overhangs (the pit is bigger on the inside) and there is a tear-shaped feature at the ventral apex of the pit (figure 3). The irregularly-shaped boss situated at the centre of the olfactory pit will also have a significant influence on its hydrodynamics.

In the second mechanism of vortex generation relevant to fish olfaction, a pair of *stable* (*i.e.* ones that are not shed) and opposing vortices are formed behind a solid cylinder as fluid flows around this cylinder, provided $10 < Re < 40$ (Lugt 1983, p. 70; Vogel 1994, p. 94 and pp. 215-218).

A likely candidate for this second type of vortex-generating mechanism is the protruding olfactory organs (equivalent to cylinders) of some puffers (figure 4), with the putative vortices either drawing water from the (wide) posterior nostril of the olfactory organ if the organ comprises an enclosed chamber on a stalk, or enhancing odorant transfer to the organ if the organ is split into two exposed folds. The Reynolds number for the olfactory organ of the blackspotted puffer (figure 4) is about 400 (Appendix A.6.7), which obviously lies outside the range quoted above for the production of a pair of stable, opposing vortices. However, it should be noted that the upper limit of this range can be increased if the cylinder is in a velocity gradient (Vogel 1994, p. 216), which it would be here since the "cylinder" is attached to the surface of the fish. It can also be increased if the cylinder is inclined in the direction of the flow (Vogel 1994, p. 216). Most interestingly, the Northern puffer, which has enclosed olfactory chambers on stalks, appears to be able to *voluntarily* bend its olfactory stalks back slightly when swimming rapidly (Copeland 1912, p. 364), behaviour in accord with the apparently voluntary trembling of the olfactory flaps of the blackspotted puffer (Section 3). In the latter, however, the olfactory organs are inclined forward (figure 4).

The third mechanism for vortex generation relevant to fish olfaction is the shedding of tip vortices from wings of finite length (Lugt 1983, p. 57; Vogel 1994, pp. 232-233). Potential candidates for shedding tip vortices in the olfactory chambers of fish are the dorsal sections of the lamellae, which are often fin-like structures with pronounced, rounded tips, particularly towards the rear of the array (see, for example, figures 5b, 5c and 10). Such vortices may act to entrain fluid through the chamber or from the olfactory lumina, in a similar manner to the proposed vortex in the olfactory chamber of the striped panchax, above.

9. CONCLUSIONS

Transport of odorant from a fish's external environment to the olfactory epithelium is mediated by several mechanisms (Table 1). These include the beating of cilia and the pumping action of one or more accessory sacs (Section 4); passage of water over or through the olfactory organ may also be induced by an external flow (Sections 5 and 8).

Each of these mechanisms can act alone or in conjunction with another one, although examples of organs that are ventilated only as the result of an external flow are apparently rare, and the organs in these cases unusual, *e.g*. the olfactory pit of a garpike or (probably) the olfactory organ of a puffer. There are likely to be several different ways in which flow through or over the organ can be generated by an external flow, including Pitot- and Venturi-like mechanisms, viscous entrainment (Section 5) and the action of vortices (Section 8). One should not rule out the possibility that, even though the beating of cilia or the pumping of an accessory sac is sufficient on their/its own to ventilate the organ, flow is also assisted by an external flow, *e.g*. through viscous entrainment from the posterior nostril. Vogel (1977b) has reported that flow through living sponges, driven by flagella within their interiors, may be assisted by an external current, so there is a precedent for a combined mechanism of this sort in Nature. In at least one case, the lemon shark (*Negaprion brevirostris*), two mechanisms – the beating of cilia and (probably) an external flow - must act cooperatively to ventilate the organ, each mechanism on its own being insufficient (Zeiske *et al.* 1987, p. 2411). The beating of cilia and the pumping action of accessory sacs in the perch and plaice (Table 1) is likely to be another example of where one mechanism complements another.

All of these mechanisms involve convection, *i.e.* the bulk movement of fluid. Convective currents within the olfactory chamber might also arise from its mechanical agitation (Section 4) or through the action of vortices, the latter generated by the pumping action of accessory sacs, or from the tips of the lamellae (Section 8).

Estimates of Reynolds number for flow generated either by the pumping action of an accessory sac or by the beating of cilia suggest that flow is laminar within the olfactory lumen (Section 6).

The final step in the transport process involves diffusion alone. The net flux of molecules (*i.e.* the diffusion current) from the aqueous phase to the olfactory epithelium depends upon the concentration gradient between the two (LaBarbera & Vogel 1982, pp. 54-56; Berg 1983, p. 18). The continuous circulation of fluid over the olfactory epithelium by the convective processes mentioned above will help maintain this concentration gradient. The steep velocity gradients generated by the beating of the cilia of any kinociliated cells present on the olfactory epithelium will also favour the diffusion process (Section 4).

One factor obstructing transport of odorant from the external environment to the olfactory organ is the boundary layer on the surface of a fish in an external flow (Section 3). The effect of the boundary layer on olfaction will be offset if the anterior nostril is placed as far forward as possible on the snout, if the olfactory organ possesses tubular anterior nostrils, if the olfactory organ protrudes from the surface of the fish on a stalk, if the fish swims fast, or if a flow of water is produced through the chamber by one of the mechanisms discussed in Sections 4 and 5.

In some instances it is not possible to say whether a particular morphological feature or action is a specific adaptation for olfaction, or whether that feature or action is a consequence of some other influence (*e.g.* development) that simply has a fortuitous, beneficial effect on olfaction. The proposed instances of mechanical agitation of the chamber (Section 4) and the forward location of the anterior nostrils in most fish (Section 5) are cases in point. What one *can* say with respect to these actions or features is that transport of odorant to the olfactory epithelium will certainly be assisted.

Some morphological features are likely to be olfactory adaptations, however. The perpendicular arrangement of anterior and posterior nostrils, with the anterior nostril directed forwards, in a continuously swimming fish (suggesting a Pitot-like mechanism for flow induction through the olfactory chamber) is one example; a flush,

rounded anterior nostril in conjunction with a slightly raised, sharp-edged posterior nostril (suggesting a Venturi-like mechanism for flow induction through the olfactory chamber) is another (Section 5).

Can one predict the appearance of a particular olfactory feature in a given situation? The following examples suggest that the answer to this question is, on balance, no.

1) The olfactory lamellae of rosettes, extended or otherwise, are generally coated, either partially or fully, with kinociliated cells (Table 1). One exception, however, is the elongated rosette of the eyed-side olfactory organ of the common sole, where kinociliated cells are absent (Holl 1965, p. 750). The principal mechanism for generating flow over the olfactory lamellae of this rosette must be the pumping action of the "two-lobed" accessory sac (Burne 1909, p. 651). Interestingly, the olfactory lamellae here are apparently attached only to the floor of the olfactory chamber (Holl 1965, figure 37), and not to its sides as is usually the case with extended rosettes (*e.g.* figure 5c). This altered arrangement might allow accessory sac-driven flow to pass over and around the lamellae in the absence of kinociliated cells.

2) It is sometimes stated (*e.g.* Nevitt 1991, p. 2) that water-pumping accessory sacs are a feature of primarily benthic (bottom-dwelling) species (*e.g.* flatfish), the ventilation provided by them allowing the fish to detect olfactory stimuli in "relatively quiet hydrodynamic microenvironments" (Webb 1993, p. 541). However, active fish (*e.g.* rainbowfish and sticklebacks) and very active fish (*e.g.* mackerel and tuna) also possess olfactory organs with water-pumping accessory sacs (Zeiske *et al.* 1979; Solger 1894; Theisen 1982; Burne 1909, p. 645; Gooding 1963). In other words, accessory sacs may be found in the olfactory organs of fish with widely differing lifestyles and habitats, both marine and freshwater. They are not confined to one particular situation.

3) Different species of fish living in the same type of environment use different mechanisms to ventilate their olfactory chambers. Thus benthic fish such as the flounder (*Platichthys flesus*) rely on water-pumping accessory sacs (Liermann 1933, pp. 15-23). Stargazers, however, rely on a respiratory flow (Atz 1952, pp. 108-109). The olfactory chambers of the angler, *Lophius piscatorius*, protrude from the dorsal

surface of the fish on stalks (Burne 1909, p. 655) and necessarily lack accessory sacs; it is therefore likely that these chambers will be ventilated either by the beating of cilia or by an externally induced flow, or both. Although it is not known whether the olfactory chambers of the angler possess kinociliated cells, the lamellae of the very similar olfactory chambers of the blackmouth angler, *Lophiomus setigerus*, which belongs to the same family, does (Yamamoto & Ueda 1978d, p. 122).

4) Similarly flow through or over the olfactory organs of fish that tend to swim continuously (*i.e*. have the same lifestyle) is not restricted to one specific mechanism. One of several is likely to operate, including a Pitot-like mechanism (probably sharks), a Venturi-like mechanism (probably the sterlet and other members of the genus *Acipenser, i.e.* sturgeons), the pumping action of an accessory sac (*e.g*. mackerel [Burne 1909, p. 645] and tuna [Gooding 1963]), or none of these (*e.g*. the garpike).

10. FUTURE DIRECTIONS

Our knowledge of the hydrodynamic processes that lead to the detection of the olfactory stimuli present in a fish's environment is limited. In no instance has flow in and around the olfactory organ of a fish been fully characterised. Clearly this is a programme that should be undertaken.

Before doing so, however, it would be advisable to have a complete anatomical (gross external and internal morphology, ultrastructure of *all* surfaces, including walls and roof) description of the olfactory organ in question. Surprisingly there are very few species of fish where this is the case. For instance, in the channel catfish, whilst the structure of the olfactory rosette and ultrastructure of the olfactory epithelium are well documented (Caprio & Raderman-Little 1978; Erickson & Caprio 1984; Morita & Finger 1998; Hansen *et al.* 2003), published information relating to key anatomical details is missing. Thus there is no information on the position of the roof of the olfactory chamber in relation to the olfactory rosette, nor on the form of this roof, nor on the distribution of kinociliated cells (if present at all) on the walls and roof of the chamber. Nor is there any information on the mucus layer (*e.g.* thickness) presumed

to coat the olfactory lamellae. In fact there is very little information on the mucus layer in any fish (Zeiske *et al.* 1976, p. 264).

Similarly there is no published information on the presence of a valve in the olfactory organ of the adult round goby. The olfactory chamber of this organ - which lacks any form of lamellar array - is lined with kinociliated cells. Intriguingly, the organ also possesses two accessory sacs (Belanger *et al*. 2003), raising the possibility that it is ventilated both by the beating of cilia *and* the pumping action of these sacs (there is precedent for such a combined mechanism in the olfactory organ of the juvenile Macculloch's rainbowfish, *Melanotaenia maccullochi* [Breucker *et al.* 1979, p. 65]). Whether these sacs are capable of pumping water through the chamber in a unidirectional fashion rests upon the presence of a valve.

As noted in Section 4, there is also very little data on the capacity of accessory sacs.

Much of this missing information may be obtained by routine anatomical techniques. However, it could be complemented by determining the anatomy of the *intact* olfactory organ by magnetic resonance imaging (Anon. 2006; Pohlmann *et al.* 2007) and X-ray microtomography (Flannery *et al.* 1987; Ritman 2004), and this data used to generate real and virtual three-dimensional models for flow visualisation (see below). For comparative purposes it would be helpful if weights and lengths of fish were routinely included in any anatomical descriptions.

Full characterisation of flow in and around the olfactory organ of a living fish would be best achieved through a combination of approaches. External flows could be monitored by laser Doppler velocimetry (Kux *et al.* 1977, 1978, 1988), particle image velocimetry (Gharib & Daribi 2000) or (possibly) by schlieren and shadowgraph techniques (Settles 2001), internal flows by magnetic resonance imaging (Bock *et al*. 2002; van der Linden *et al*. 2004; Pohlmann *et al.* 2007). These experiments would not be trivial, however, especially if one were keen not to cause the fish distress. Using accurate plastic models, or performing computational fluid dynamics (Versteeg & Malalasekera 2007) on virtual models (Yang *et al.* 2007), may be more pragmatic approaches in the first instance, at least in some cases.

Several subjects for the hydrodynamics experiments are indicated in Table 1, but might also include the blackspotted puffer. They are suggested on the basis that they could be used to explore some of the tentative ideas presented in this article, including the role of an external flow in inducing flow (by Pitot-like or Venturi-like mechanisms) over or through the olfactory organ (and whether external flows augment the pumping action of cilia or accessory sacs) and the presence of vortices in and around the olfactory organ. Particularly attractive subjects, missing anatomical data notwithstanding, are the channel catfish and goldfish, since there are a considerable amount of data on the ultrastructure of the olfactory epithelium in these species (*e.g.* Caprio & Raderman-Little 1978; Erickson & Caprio 1984; Hansen *et al.* 1999), and the expression of odorant receptors within the olfactory epithelium (*e.g.* Ngai *et al.* 1993; Morita & Finger 1998; Hansen *et al.* 2003, 2004). It would also be of interest to compare the energy expended in pumping water through the olfactory chamber in the different species. Pike and sterlet have been suggested as subjects for hydrodynamic studies on the basis of a possible Venturi-like mechanism, but also because of the effect their contrasting lifestyles might have on the form and positioning of their nostrils.

Another interesting comparison would be the hydrodynamics of the olfactory organs of the garpike and longnose gar. Both species are similar in shape, with elongated bodies and jaws (*cf.* figures on p. 85 and p. 266 of Nelson [1993])[4]. Both inhabit very different environments and have different lifestyles: the longnose gar is a typically rather inactive freshwater fish (Werner 2004, p. 59) that prefers sluggish waters (Ross 2001, p. 84); the garpike, on the other hand, is a very active (Theisen *et al*. 1980, p. 169), primarily oceanic fish (Wheeler 1969, p. 237). The olfactory organs of the longnose gar are paired chambers situated on the tip of the snout. The olfactory organs of the garpike, however, are exposed and situated at the base of the snout (figure 3).

Two miscellaneous but nevertheless important issues might be investigated. The first is the role of kinociliated cells in the zebrafish olfactory chamber. Do they propel

[4] Although both are ray-finned fishes, they belong to different orders.

mucus, or water, or both? The second is whether or not the trembling of the olfactory stalks of the blackspotted puffer serves an olfactory purpose.

Some topics have not been covered in this article, but merit attention. These include the hydrodynamics of tubular nostrils (both anterior and posterior), the function of secondary folds on the olfactory lamellae and the limitations on the number of lamellae in a particular type of olfactory array. One might think that these matters are straightforward. For example, the function of the secondary folds surely is to increase the sensory surface area. This might be the case in sharks, where the olfactory epithelium does indeed coat the secondary folds (Theisen *et al.* 1986, p. 77), but this cannot be true for those fish in which secondary folds are not coated with olfactory epithelium, *e.g.* the jarbua terapon, *Terapon jarbua* (Yamamoto & Ueda 1979b, p. 278). In this case the secondary folds appear similar to the ridges in the green swordtail and striped panchax, in which olfactory epithelium is also absent (compare Zeiske 1973, figure 3 and Zeiske 1974, figure 3*c* with Bashor *et al.* 1974, figure 2*b*). Zeiske (1974, pp. 45-46) has commented further on this point.

Finally, Settles (2005, pp. 205-206) has advocated the olfactory organs of fish as models on which to base an artificial sensor, or at least the architecture of one, on the basis that they are compact and generally perform one function only – olfaction. The principal ventilation mechanism in the particular example cited by Settles, the olfactory organ of the European eel, is likely to be the beating of cilia (Teichmann 1959, p. 240). Since there is as yet no artificial equivalent of kinociliated cells, a better immediate choice of model may be an olfactory organ ventilated primarily by an accessory sac, the pumping action of which could very easily be replicated by an artificial pump. Examples of such olfactory organs include that of the sea lamprey or the striped panchax (Table 1). A device based on one of these organs would lend itself to a sniffing-like action too.

ACKNOWLEDGEMENTS

I thank the following people for help in compiling the manuscript: Phil Crabb and James Maclaine (Natural History Museum, London); Anne Hansen (University of

Colorado); Aidan Neeson (Bristol Zoo Gardens); Xavier Mear, Jacky Rawlings, Felicity Veazey and Bridget Baker (University of Bath); Peter Smith (Environment Agency, UK); Jürgen Kux and Eckart Zeiske (University of Hamburg); Gabrielle Nevitt (University of California, Davis); Robert Holbrook (University of Oxford). I also thank Jos Darling, Steven Vogel, Anne Hansen, Richard Bomphrey and three anonymous referees for valuable comments on the manuscript. The Defence Science and Technology Laboratory provided financial support. This work was carried out as part of the Electronics Systems Research Programme for the MOD Research Acquisition Organisation. The article itself was prompted by reading Settles (2005).

REFERENCES

Alexander, R. McN. 1965 Structure and function in the catfish. *J. Zool*. **148**, 88-152.

Alioto, T. S. & Ngai, J. 2005 The odorant receptor repertoire of teleost fish. *BMC Genomics* **6**, Art. No. 173. DOI 10.1186/1471-2164-6-173

Anderson, E. J., McGillis, W. R. & Grosenbaugh, M. A. 2001 The boundary layer of swimming fish. *J. Exp. Biol.* **204**, 81-102.

Anon. 2006 Fish images provide net benefit to researchers. *Nature* **440**, 397. DOI 10.1038/440396a

Atema, J. 1988 Distribution of chemical stimuli. In *Sensory biology of aquatic animals* (eds. J. Atema, R. R. Fay, A. N. Popper & W. N. Tavolga), pp. 29-56. New York: Springer-Verlag.

Atz, J. W. 1952 Internal nares in the teleost, *Astroscopus*. *Anat. Rec.* **113**, 105-115.

Baker, C. F. & Montgomery, J. C. 1999 The sensory basis of rheotaxis in the blind Mexican cave fish, *Astyanax fasciatus*. *J. Comp. Physiol.* A **184**, 519-527.

Balsam, W. L. & Vogel, S. 1973 Water movement in Archaeocyathids. *J. Paleontology* **47**, 979-984.

Bashor, D. P., Beuerman, R. W. & Easton, D. M. 1974 Ciliary action and normal movement of odorant wavefronts in garfish nasal capsule of *Lepisosteus osseus*. *Experientia* **30**, 777-779.

Bateson, W. 1890 The sense-organs and perceptions of fishes. *J. Marine Biol. Assoc.* **1**, 225-256.

Beamish, F. W. H. 1978 Swimming capacity. In *Fish physiology Vol. VII* (eds. W. S. Hoar & D. J. Randall), pp. 101-187. New York: Academic Press.

Bejan, A. 1993 *Heat transfer*. New York: John Wiley.

Belanger, R. M., Smith, C. M., Corkum, L. D. & Zielinski, B. S. 2003 Morphology and histochemistry of the peripheral olfactory organ in the round goby, *Neogobius melanostomus* (Teleostei: Gobiidae). *J. Morph.* **257**, 62-71.

Berg, H. C. 1983 *Random walks in biology*. Princeton: Princeton University Press.

Bjerselius, R. & Olsén, K. H. 1993 A study of the olfactory sensitivity of crucian carp (*Carassius carassius*) and goldfish (*Carassius auratus*) to 17α,20β-dihydroxy-4-pregnen-3-one and prostaglandin $F_{2\alpha}$. *Chem. Senses* **18**, 427-436.

Bock, C., Sartoris, F.- J. & Pörtner, H.-O. 2002 *In vivo* MR spectroscopy and MR imaging on non-anaesthetized marine fish. *Magn. Reson. Imaging* **20**, 165-172.

Breucker, H., Zeiske, E. & Melinkat, R. 1979 Development of the olfactory organ in the rainbow fish *Nematocentris maccullochi* (Atheriniformes, Melanotaeniidae). *Cell Tissue Res.* **200**, 53-68.

Burne, R. H. 1909 The anatomy of the olfactory organ of Teleostean fishes. *Proc. Zool. Soc. Lond*. 610-663.

Cameron, J. N. & Cech, J. J. 1970 Notes on the energy cost of gill ventilation in teleosts. *Comp. Biochem. Physiol.* **34**, 447-455.

Cancalon, P. 1978 Isolation and characterisation of the olfactory epithelial cells of the catfish. *Chem. Senses & Flavour* **3**, 381-396.

Caprio, J. & Raderman-Little, R. 1978 Scanning electron microscopy of the channel catfish olfactory lamellae. *Tissue & Cell* **10**, 1-9.

Chen, X.- Y. & Arratia, G. 1994 Olfactory organ of Acipenseriformes and comparison with other Actinopterygians. *J. Morph*. **222**, 241-267.

Copeland, M. 1912 The olfactory reactions of the puffer or swellfish, *Spheroides maculatus* (Bloch and Schneider). *J. Exp. Biol.* **12**, 363-368.

Cussler, E. L. 1997 *Diffusion*, 2nd edn. Cambridge: Cambridge University Press.

Denny, M. W. 1993 *Air and water*. Princeton: Princeton University Press.

Døving, K. B., Dubois-Dauphin, M., Holley, A. & Jourdan, F. 1977 Functional anatomy of the olfactory organ of fish and the ciliary mechanism of water transport. *Acta Zool.* **58**, 245-255.

Dubois, A. B., Cavagna, G. A. & Fox, R. S. 1974 Pressure distribution on the body surface of swimming fish. *J. Exp. Biol.* **60**, 581-591.

Eaton, T. H. 1956 Notes on the olfactory organs in Centrarchidae. *Copeia* No. 3, 196-199.

Erickson, J. R. & Caprio, J. 1984 The spatial distribution of ciliated and microvillous olfactory receptor neurons in the channel catfish is not matched by a differential specificity to amino acid and bile salt stimuli. *Chem. Senses* **9**, 127-141.

Flannery, B. P., Deckman, H. W., Roberge, W. G. & D'Amico, K. L. 1987 Three-dimensional X-ray microtomography. *Science* **237**, 1439-1444.

Gharib, M. & Daribi, D. 2000 Digital particle image velocimetry. In *Flow visualization* (eds. A. J. Smits & T. T. Lim), pp. 123-147. London: Imperial College Press.

Gooding, R. M. 1963 The olfactory organ of the skipjack *Katsuwonus pelamis*. *FAO Fisheries Reports* **3**, 1621-1631.

Hamdani, E. H., Lastein, S., Gregersen, F. & Døving, K. B. 2006 Seasonal variations in the appearance of crypt cells in the olfactory epithelium of the Crucian carp. *Chem. Senses* **31**, E54.

Hamdani, E. H. & Døving, K. B. 2007 The functional organization of the fish olfactory system. *Prog. Neurobiol.* **82**, 80-86. DOI 10.1016/j.pneurobio.2007.02.007

Hansen, A. & Zeiske, E. 1998 The peripheral olfactory organ of the zebrafish, *Danio rerio*. *Chem. Senses* **23**, 39-48.

Hansen, A., Zippel, H. P., Sorensen, P. W. & Caprio, J. 1999 Ultrastructure of the olfactory epithelium in intact, axotomized, and bulbectomized goldfish, *Carassius auratus*. *Microscopy Res. Tech.* **45**, 325-338.

Hansen, A., Rolen, S. H., Anderson, K., Morita, Y., Caprio, J. & Finger, T. E. 2003 Correlation between olfactory receptor cell type and function in the channel catfish. *J. Neuroscience* **23**, 9328-9339.

Hansen, A., Anderson, K. T. & Finger, T. E. 2004 Differential distribution of olfactory receptor neurons in goldfish. *J. Comp. Neurol*. **477**, 347-359. DOI 10.1002/cne.20202.

Hansen, A. & Zielinski, B. S. 2005 Diversity in the olfactory epithelium of bony fishes. *J. Neurocytology* **34**, 183-208. DOI 10.1007/s11068-005-8353-1.

Holl, A. 1965 Vergleichende Morphologische und Histologische Untersuchungen am Geruchsorgan der Knochenfische (Comparative morphological and histological studies on the olfactory organs of bony fish). *Z. Morph. Ökol. Tiere* **54**, 707-782. (In German.)

Holl, A. & Meinel, W. 1968 The olfactory organ of the deep-sea fish *Aphanopus carbo* (Percomorphi, Trichiuridae). *Helgoländer wiss. Meeresunters.* **18**, 404-423. (In German, with an English summary.)

Holl, A., Schulte, E. & Meinel, W. 1970 Functional morphology of the olfactory organ and histology of the head appendages of the moray eel *Rhinomuraena ambonensis* (Teleostei, Anguilliformes). *Helgoländer wiss. Meeresunters.* **21**, 103-123. (In German, with an English summary.)

Hughes, G. M. 1960 A comparative study of gill ventilation in marine teleosts. *J. Exp. Biol.* **37**, 28-45.

Jahn, T. L. & Votta, J. J. 1972 Locomotion of Protozoa. *Ann. Rev. Fluid Mech.* **4**, 93-116.

Johansen, K. & Hol, R. 1960 A cineradiographic study of respiration in *Myxine glutinosa* L. *J. Exp. Biol.* **37**, 474-480.

Kapoor, A. S. & Ojha, P. P. 1973 Functional anatomy of the nose and accessory nasal sacs in the teleost *Channa punctatus* Bloch. *Acta Anat.* **84**, 96-105.

Kerstens, A., Lomholt, J. P. & Johansen, K. 1979 The ventilation, extraction and uptake of oxygen in undisturbed flounders, *Platichthys flesus*. *J. Exp. Biol.* **83**, 169-179.

Kleerekoper, H. & van Erkel, G. A. 1960 The olfactory apparatus of *Petromyzon marinus* L. *Can. J. Zool.* **38**, 209-223.

Kleerekoper, H. 1969 *Olfaction in fishes*. Bloomington: Indiana University Press.

Kux, J., Lammers, G., Melinkat, R. & Zeiske, E. 1977 Measurement of the velocity at the nares of the olfactory organ of fishes with a laser velocimeter. In *Photon correlation spectroscopy and velocimetry* (eds. H. Z. Cummins & E. R. Pike), pp. 492-494. New York: Plenum.

Kux, J., Zeiske, E. & Melinkat, R. 1978 Measurement of flow velocity at the nares of the olfactory organ of fishes with a laser-velocimeter. *LASER/Elektro-Optik* **10**, 21. (In German, with an English summary.)

Kux, J., Zeiske, E. & Osawa, Y. 1988 Laser Doppler velocimetry measurement in the model flow of a fish olfactory organ. *Chem. Senses* **13**, 257-265.

LaBarbera, M. & Vogel, S. 1982 The design of fluid transport systems in organisms. *Am. Sci.* **70**, 54-60.

Lide D. R. 2004 *CRC Handbook of Chemistry and Physics*, 85th edn. Boca Raton: CRC Press.

Liermann, K. 1933 Über den Bau des Geruchsorgans der Teleostier (The structure of the olfactory organ in Teleosts). *Z. Anat.* **100**, 1-39. (In German.)

Lim, T. T. 2000 Dye and smoke visualization. In *Flow visualization* (eds. A. J. Smits & T. T. Lim), pp. 43-72. London: Imperial College Press.

Lugt, H. J. 1983 *Vortex flow in Nature and technology*. New York: John Wiley.

Massey, B. S. 1989 *Mechanics of fluids*, 6th edn. London: Van Nostrand Reinhold.

Melinkat, R. & Zeiske, E. 1979 Functional morphology of ventilation of the olfactory organ in *Bedotia geayi* Pellegrin 1909 (Teleostei, Atherinidae). *Zool. Anz*. **203**, 354-368.

Morita, Y. & Finger, T. E. 1998 Differential projections of ciliated and microvillous olfactory receptor cells in the catfish, *Ictalurus punctatus*. *J. Comp. Neurol.* **398**, 539-550.

Murphy, C. A., Stacey, N. E. & Corkum, L. D. 2001 Putative steroidal pheromones in the round goby, *Neogobius melanostomus*: olfactory and behavioral responses. *J. Chem. Ecol.* **27**, 443-470.

Nelson, J. S. 1994 *Fishes of the world*, 3rd edn. New York: Wiley.

Nevitt, G. A. 1991 Do fish sniff? A new mechanism of olfactory sampling in pleuronectid flounders. *J. Exp. Biol.* **157**, 1-18.

Ngai, J., Chess, A., Dowling, M. M., Necles, N., Macagno, E. R. & Axel, R. 1993 Coding of olfactory information: topography of odorant receptor expression in the catfish olfactory epithelium. *Cell* **72**, 667-680.

Nielsen, N. F., Larsen, P. S., Riisgård, H. U. & Jørgensen, C. B. 1993 Fluid motion and particle retention in the gill of *Mytilus edulis*. *Marine Biology*, **116**, 61-71.

Nikonov, A. A., Finger, T. E. & Caprio, J. 2005 Beyond the olfactory bulb: an odotopic map in the forebrain. *Proc. Natl. Acad. Sci. USA* **102**, 18688-18693. DOI 10.1073/pnas.0505241102

Norman, J. R. 1934 *A systematic monograph of the flatfishes (Heterosomata)*, Vol. I. London: British Museum.

Ojha, P. P. & Kapoor, A. S. 1972 Functional anatomy of [the] nose in the teleost *Wallago attu* Bl. & Schn. *Arch. Biol. (Liège)* **83**, 105-116.

Ojha, P. P. & Kapoor, A. S. 1974 Structure and function of the olfactory organs in the fish *Sisor rabdophorus* Ham. *Acta Anat.* **87**, 124-130.

Orcutt, H. G. 1950 The life history of the starry flounder *Platichthys stellatus* (Pallas). *State of California Department of Natural Resources Division of Fish and Game Bureau of Marine Fisheries, Fish Bulletin No. 78*, 1-68.

Pfeiffer, W. 1964 The morphology of the olfactory organ of *Hoplopagrus guentheri* Gill 1862. *Can. J. Zool.* **42**, 235-237.

Pfeiffer, W. 1968 The olfactory organ of the Polypteridae (Pisces, Brachiopterygii). *Z. Morph. Tiere* **63**, 75-110. (In German, with an English summary.)

Pohlmann, K., Grasso, F. W. & Breithaupt, T. 2001 Tracking wakes: the nocturnal predatory strategy of piscivorous catfish. *Proc. Natl. Acad. Sci. USA* **98**, 7371-7374. DOI 10.1073/pnas.121026298

Pohlmann, A., Möller, M., Decker, H. & Schreiber, W. G. 2007 MRI of tarantulas: morphological and perfusion imaging. *Magn. Reson. Imaging* **25**, 129-135. DOI 10.1016/j.mri.2006.08.019

Ritman, E. L. 2004 Micro-computed tomography – current status and developments. *Ann. Rev. Biomed. Eng*. **6**, 185-208. DOI 10.1146/annurev.bioeng.6.040803.140130

Ross, S. T. 2001 *Inland fishes of Mississippi.* Singapore: University Press of Mississippi.

Sattler, W. & Kracht, A. 1963 Drift-Fang einer Trichopterenlarve unter Ausnutzung der Differenz von Gesamtdruck und statischem Druck des fliessenden Wassers. (Drift capture by a *Trichoptera* larva through the utilisation of the difference in total pressure and static pressure of the flowing water.) *Naturwissen.* **50**, 362. (In German.)

Schmidt-Nielsen, K. 1997 *Animal physiology*, 5th edn. Cambridge: Cambridge University Press.

Schulte, E. & Holl, A. 1971 Ultrastructure of the olfactory epithelium of *Calamoichthys calabaricus* J. A. Smith (Pisces, Brachiopterygii). *Z. Zellforsch.* **120**, 261-279. (In German, with an English summary.)

Schulte, E. 1972 Studies of the *regio olfactoria* in the eel, *Anguilla anguilla*. *Z. Zellforsch*. **125**, 210-228. (In German, with an English summary.)

Schulte, E. & Riehl, R. 1978 Ultrastructure of the *regio olfactoria* of the piranha *Serrasalmus nattereri* (Kner, 1860) (Teleostei, Characidae). *Zool. Anz.* **200**, 119-131. (In German, with an English summary.)

Settles, G. S. 2001 *Schlieren and shadowgraph techniques*. Berlin: Springer.

Settles, G. S. 2005 Sniffers: fluid-dynamic sampling for olfactory trace detection in Nature and homeland security. *J. Fluids Eng.* **127**, 189-218.

Shaw, R. 1960 The influence of hole dimensions on static pressure measurements. *J. Fluid Mech.* **7**, 550-564.

Sleigh, M. A. 1978 Fluid propulsion by cilia and flagella. In *Comparative physiology: water, ions and fluid mechanics* (eds. K. Schmidt-Nielsen, L. Bolis & S. H. P. Maddrell), pp. 255-266. Cambridge: Cambridge University Press.

Sleigh, M. A. 1989 Adaptions of ciliary systems for the propulsion of water and mucus. *Comp. Biochem. Physiol.* **94A**, 359-364.

Solger, B. 1894 Notiz über die Nebenhöhle des Geruchsorgans von *Gasterosteus aculeatus* L. (Note on the adjacent chambers of the olfactory organs of *Gasterosteus aculeatus* L.). *Z. Wiss. Zool.* **57**, 186. (In German.)

Steffensen, J. F., Lomholt, J. P. & Johansen, K. 1982 Gill ventilation and O_2 extraction during graded hypoxia in two ecologically distinct species of flatfish, the flounder (*Platichthys flesus*) and the plaice (*Pleuronectes platessa*). *Env. Biol. Fish*. **7**, 157-163.

Steffensen, J. F. & Lomholt, J. P. 1983 Energetic cost of active branchial ventilation in the sharksucker, *Echeneis naucrates*. *J. Exp. Biol.* **103**, 185-192.

Stoddart, D. M. 1980 *The ecology of vertebrate olfaction*. London: Chapman & Hall.

Strahan, R. 1958 The velum and the respiratory current of *Myxine*. *Acta Zool.* **39**, 227-240.

Teichmann, H. 1954 Vergleichende Untersuchungen an der Nase der Fische (Comparative studies on the nose of fish). *Z. Morph. Ökol. Tiere* **43**, 171-212. (In German.)

Teichmann, H. 1959 Über die Leistung des Geruchssinnes beim Aal [*Anguilla anguilla* (L.)] (On the performance of the sense of smell of the eel). *Z. für vergleichende Physiologie* **42**, 206-254.

Teyke, T. 1985 Collision with and avoidance of obstacles by blind cave fish *Anoptichthys jordani* (Characidae). *J. Comp. Physiol. A* **157**, 837-843.

Theisen, B. 1970 The morphology and vascularization of the olfactory organ in *Calamoichthys calabaricus* (Pisces, Polypteridae). *Vidensk. Meddr. dansk naturh. Foren.* **133**, 31-50.

Theisen, B. 1973 The olfactory system of the hagfish *Myxine glutinosa*. *Acta Zool*. **54**, 271-284.

Theisen B., Breucker, H., Zeiske, E. & Melinkat, R. 1980 Structure and development of the olfactory organ in the garfish *Belone belone* (L.) (Teleostei, Atheriniformes). *Acta Zool.* **61**, 161-170.

Theisen, B. 1982 Functional morphology of the olfactory organ in *Spinachia spinachia* (L.) (Teleostei, Gasterosteidae). *Acta Zool.* **63**, 247-254.

Theisen, B., Zeiske, E. & Breucker, H. 1986 Functional morphology of the olfactory organs in the spiny dogfish (*Squalus acanthias* L.) and the small-spotted catshark (*Scyliorhinus canicula* L.). *Acta Zool.* **67**, 73-86.

Theisen, B., Zeiske, E., Silver, W.L., Marui, T. & Caprio, J. 1991 Morphological and physiological studies on the olfactory organ of the striped eel catfish, *Plotosus lineatus*. *Marine Biology*, **110**, 127-135.

Van der Linden, A., Verhoye, M., Pörtner, H. O. & Bock, C. 2004 The strengths of *in vivo* magnetic resonance imaging (MRI) to study environmental adaptational physiology in fish. *Magnetic Resonance Materials in Physics, Biology and Medicine* **17**, 236-248. DOI 10.1007/s10334-004-0078-0

Versteeg, H. K. & Malalasekera, W. 2007 *An introduction to computational fluid dynamics*, 2nd edn. Harlow: Pearson Education.

Vogel, S. & Bretz, W. L. 1972 Interfacial organisms: passive ventilation in the velocity gradients near surfaces. *Science*, **175**, 210-211.

Vogel, S., Ellington, C. P. & Kilgore, D. L. 1973 Wind-induced ventilation of the burrow of the prairie-dog, *Cynomys ludovicianus*. *J. Comp. Physiol.* **85**, 1-14.

Vogel, S. 1974 Current-induced flow through the sponge, *Halichondria*. *Biol. Bull.* **147**, 443-456.

Vogel, S. 1977a Flows in organisms induced by movements of the external medium. In *Scale effects in animal locomotion* (ed. T. J. Pedley), pp. 285-297. London: Academic Press.

Vogel, S. 1977b Current-induced flow through living sponges in nature. *Proc. Natl. Acad. Sci. USA* **74**, 2069-2071.

Vogel, S. 1978 Organisms that capture currents. *Sci. Am.* **239** (August), 108-117.

Vogel, S. 1994 *Life in moving fluids*, 2nd edn. Princeton: Princeton University Press.

Vogel, S. 2004 Living in a physical world. *J. Biosci.* **29**, 391-397.

Waldschmidt, J. 1887 Beitrag zur Anatomie des Zentralnervensystems und des Geruchsorgans von *Polypterus bichir* (On the anatomy of the central nervous systems and the olfactory organs of *Polypterus bichir*). *Anat. Anz*. **2**, 308-322. (In German.)

Wallace, J. B. & Sherberger, F. F. 1975 The larval dwelling and feeding structure of *Macronema transversum* (Walker) (Trichoptera: Hydropsychidae). *Anim. Behav.* **23**, 592-596.

Webb, J. F. 1993 The accessory nasal sacs of flatfishes. *Bull. Marine Sci*. **52**, 541-553.

Werner, R. G. 2004 *Freshwater fishes of the Northeastern United States*. Syracuse: Syracuse University Press.

Wheeler, A. 1969 *The fishes of the British Isles and North-West Europe*. London: MacMillan.

Wiedersheim, R. 1887 Über rudimentäre Fischnasen (On rudimentary fish noses). *Anat. Anz*. **2**, 652-657. (In German.)

Yamamoto, M. & Ueda, K. 1977 Comparative morphology of fish olfactory epithelium - I Salmoniformes. *Bull. Jap. Soc. Sci. Fish.* **43**, 1163-1174.

Yamamoto, M. & Ueda, K. 1978a Comparative morphology of fish olfactory epithelium - III Cypriniformes. *Bull. Jap. Soc. Sci. Fish.* **44**, 1201-1206.

Yamamoto, M. & Ueda, K. 1978b Comparative morphology of fish olfactory epithelium - IV Anguilliformes and Myctophiformes. *Bull. Jap. Soc. Sci. Fish.* **44**, 1207-1212.

Yamamoto, M. & Ueda, K. 1978c Comparative morphology of fish olfactory epithelium - VI Siluriformes. *Zool. Mag. (Zool. Soc. Jap.)* **87**, 254-261.

Yamamoto, M. & Ueda, K. 1978d Comparative morphology of fish olfactory epithelium - VII Gadiformes, Lophiiformes and Gobiesociformes. *J. Fac. Sci. Tokyo Uni.* **14**, 115-125.

Yamamoto, M. & Ueda, K. 1979a Comparative morphology of fish olfactory epithelium - IX Tetraodontiformes. *Zool. Mag. (Zool. Soc. Jap.)* **88**, 210-218.

Yamamoto, M. & Ueda, K. 1979b Comparative morphology of fish olfactory epithelium - X Perciformes, Beryciformes, Scorpaeniformes, and Pleuronectiformes. *J. Fac. Sci. Tokyo Uni.* **14**, 273-297.

Yamamoto, M. 1982 Comparative morphology of the peripheral olfactory organ in teleosts. In *Chemoreception in fishes* (ed. T. J. Hara), pp. 39-59. Amsterdam: Elsevier.

Yang, G. C., Scherer, P. W. & Mozell, M. M. 2007 Modeling inspiratory and expiratory steady-state velocity fields in the Sprague-Dawley rat nasal cavity. *Chem. Senses* **32**, 215-223. DOI 10.1093/chemse/bjl047

Zeiske, E. 1973 Morphological studies on the olfactory organs of cyprinodontoid fishes (Pisces, Cyprinodontoidea). *Z. Morph. Tiere* **74**, 1-16. (In German, with an English summary.)

Zeiske, E. 1974 Morphological and morphometric studies on the olfactory organs of oviparous cyprinodont fishes (Pisces). *Z. Morph. Tiere* **77**, 19-50. (In German, with an English summary.)

Zeiske, E., Melinkat, R., Breucker, H. & Kux, J. 1976 Ultrastructural studies on the epithelia of the olfactory organ of cyprinodonts (Teleostei, Cyprinodontoidea). *Cell Tiss. Res*. **172**, 245-267.

Zeiske, E, Breucker, H. & Melinkat, R. 1979 Gross morphology and fine structure of the olfactory organ of rainbow fish (Atheriniformes, Melanotaeniidae). *Acta Zool.* **60**, 173-186.

Zeiske, E., Theisen B. & Gruber, S. H. 1987 Functional morphology of the olfactory organ of two carcharhinid shark species. *Can. J. Zool.* **65**, 2406-2412.

Zeiske, E., Theisen, B. & Breucker, H. 1992 Structure, development, and evolutionary aspects of the peripheral olfactory system. In *Fish chemoreception* (ed. T. J. Hara), pp. 13-39. London: Chapman & Hall.

Zeiske, E., Theisen, B. & Breucker, H. 1994 The olfactory organ of the hardhead sea catfish, *Arius felis* (L.). *Acta Zool.* **75**, 115-123.

Zeiske, E., Kasumyan, A., Bartsch, P. & Hansen, A. 2003 Early development of the olfactory organ in sturgeons of the genus *Acipenser*. *Anat. Embryol.* **206**, 357-372. DOI 10.1007/s00429-003-0309-6.

FIGURE CAPTIONS

Figure 1. Photograph of the head of a preserved Northern pike (*Esox lucius*) specimen (total length 17 cm), lateral (left-hand side) aspect. Boxed region highlights the anterior (A) and posterior nostrils (P). Scale bar: 1 cm. Inset: boxed region from main photograph. Scale bar 1 mm. Photograph copyright Natural History Museum, London (specimen catalogue number BMNH 1963.4.26:1-2).

Figure 2. Schematic showing the main features of the olfactory organ of a Northern pike (longitudinal cross-section). The olfactory chamber is shaded light grey. This particular chamber includes an internal flap (F) believed to direct flow onto the sensory area (Burne 1909, p. 629). The latter is located between the low ridges, and at the centre of the radial arrangement formed by the ridges. In fact, the ridge system is more complicated than shown, with minor ridges lying between major ridges, and transverse ridges connecting the major and minor ridges, giving a cobweb-like structure, with the sensory region occupying the spaces in the cobweb (Holl 1965, pp. 738-740). Schematic based on Text-fig. 198 of Burne (1909) and figure 21 of Teichmann (1954).

Figure 3. Photograph of the preserved head of a garpike, *Belone belone*, highlighting the triangular olfactory pit (boxed region). The olfactory epithelium coats both boss and pit (Theisen *et al.* 1980, figure 2*d*). Scale bar: 1 cm. Inset: boxed region from main photograph. Scale bar: 250 μm. Photographs copyright Natural History Museum, London (specimen catalogue number BMNH 2005.4.27:24-30).

Figure 4. Photograph of a live blackspotted puffer, *Arothron nigropunctatu*s (normal phase). The olfactory organs are the pair of dark, forked structures lying within the boxed region. Inset: boxed region from main photograph. Scale bar *ca.* 3 mm. Photograph courtesy of Bristol Zoo Gardens, UK.

Figure 5. Three different types of olfactory lamellar array. (*a*) Longitudinal array of olfactory lamellae. Top: photograph of lateral aspect of head of a preserved specimen of a male angler fish (*Linophryne* species, total length 22 mm). Photograph copyright

Natural History Museum, London (specimen catalogue number BMNH 2004.11.6.44). Bottom: plan view of olfactory chamber. Scale bar: 1 mm. *(b)* Rosette. Top: electron micrograph of olfactory chamber of goldfish, *Carassius auratus*. Reprinted with permission of Wiley-Liss, Inc., a subsidiary of John Wiley & Sons, Inc. from Hansen *et al.* (2004). Copyright 2004 John Wiley & Sons, Inc. Scale bar: 0.3 mm. Bottom: plan view. *(c)* Elongated rosette. Top: electron micrograph of olfactory chamber of European eel, *Anguilla anguilla*. Note that the raphe is gently curved rather than straight. Scale bar: 1 mm. Reproduced with permission of Springer Science + Business Media, LLC from Hansen & Zielinski (2005). Copyright 2006 Springer Science + Business Media, LLC. Bottom: Plan view of olfactory chamber. A and P: outlines/positions of anterior and posterior nostrils, respectively; d: distance between successive olfactory lamellae (referred to here as the depth of the olfactory lumen). The arrows in figures 5*b* and 5*c* highlight the rounded fin-like extremities of the lamellae, potential candidates for shedding tip vortices (Section 8).

Figure 6. Comparison of velocity profiles for fully developed flow between two wide but closely spaced parallel plates (P) and within a circular pipe (C). Flow between the parallel plates is, on the average, closer to the walls of the channel (CH) than in a circular pipe, given that the channels are of the same length, the diameter of the circular pipe is equal to the perpendicular distance between the two parallel plates, and the fluid flowing through them has the same viscosity. The vertical lines below d_P and d_C show the average distances of the flow from the wall of the parallel plate channel and the circular pipe, respectively. Arrow: direction of flow. Filled circles indicate that the velocity at the wall is zero (the no-slip condition [Vogel 1994, pp. 18-20]).

Figure 7. Boundary layers associated with swimming fish. The boundary layers indicated (shaded) are highly schematic, and are of course shown in two-dimensions only. The relative motion of the fish with respect to the water (arrow) in each case is from right to left. *(a)* Profile of the head of a haddock (*Melanogrammus aeglefinus*) from a drawing (Wheeler 1969, p. 277). Approximate location of olfactory organ indicated by the filled oval. *(b)* Profile of the head of a bichir (*Polypterus endlicheri*) based on video footage of a swimming fish at Bristol Zoo Gardens, UK. Only the left-hand tubular anterior nostril is apparent (black). *(c)* Profile of head of blackspotted

puffer taken from video footage of a swimming fish at Bristol Zoo Gardens, UK. Only the left-hand olfactory organ is apparent (black). Diagrams not to scale.

Figure 8. Schematic longitudinal cross-section through the olfactory organ of an "oviparous cyprinodont" fish (Zeiske 1974), a group to which the striped panchax belongs. Based on figure 3*a* of Kux *et al.* 1988, the same cross-section through the green swordtail is likely to be similar. Figure redrawn from figure 1 of Zeiske 1974.

Figure 9. Main pictures: photographs of the head of a preserved specimen of a sterlet, *Acipenser ruthenus* (total length *ca.* 35 cm). *(a)* Lateral view, showing anterior and posterior nostrils of left-hand olfactory organ. Inset: photograph of the anterior and posterior nostrils of the olfactory organ of a lake sturgeon, *Acipenser fulvescens* (total length *ca*. 25 cm), highlighting the well-rounded rim of the anterior nostril (arrowhead). The posterior nostril of this particular organ is, unusually for sturgeons, partially occluded by a flap of skin (F); the posterior nostril of the other olfactory organ of this specimen was the more typical oval hole. Scale bar: 5 mm. (*b*) Dorsal view. Note the protruding posterior nostril. Scale bar: 1 cm. Scale for both (*a*) and (*b*) is the same. A: anterior nostril; P: posterior nostril. Photographs courtesy of the Natural History Museum [specimen catalogue numbers BMNH 1896.10.3.53-54 (*Acipenser ruthenus*) and BMNH 1963.10.28.5 (*Acipenser fulvescens*)].

Figure 10. Schematic of part of the elongated olfactory rosette of the channel catfish, *Ictalurus punctatus*. Lamellae are attached to the raphe, and to the floor and sides of the olfactory chamber (dotted lines). The roof of the chamber is not shown in the main picture but is shown in the inset. The free edges of the lamellae protrude into the channel (grey in inset) above the array. There is no information in the literature on the nature of this channel, though based on the anatomy of other fish with similar olfactory organs (*e.g*. the European eel [Teichmann 1959, p. 241] and the catfish *Wallago attu* [Ojha & Kapoor 1972, pp. 108-110]), the channel is probably narrow. The arrow above the array indicates the direction of flow in this channel. The sensory areas of the two nearest lamellar faces are shown in grey (only the sensory area on the nearest pair of lamellar faces is shown, for convenience); the remaining lamellar area is predominantly occupied by kinociliated cells. The curved arrows indicate the approximate direction of flow over the lamellae. Again, there is no information in the

literature on the direction of flow over the olfactory lamellae of the channel catfish, and the direction shown here is an assumption based on the location of the kinociliated cells. Flow is only shown on the nearest pair of lamellar faces, but will be similarly directed over the other lamellar faces in the array. The fin-like dorsal regions (filled circles) of each lamella are potential candidates for shedding tip vortices (Section 8). Scale bar: 0.5 mm. The schematic is based on figure 1 of Erickson & Caprio 1984.

Figure 11. Schematic showing how water expelled from a single accessory sac (large arrow) could cause a vortex (circular arrow) at the back of the olfactory chamber of a fish, leading to enhanced odorant transfer and possible entrainment of fluid through the anterior nostril (long arrow). Adapted from figure 1 of Zeiske 1974. See also figure 8.

TABLE CAPTIONS

Table 1. Ventilation mechanisms in the olfactory organs of fish. Species have been included in the table on the basis that the gross morphology and fine structure of their olfactory organs has been reasonably well characterised. Species are grouped according to the mechanisms thought to be ventilating their olfactory organs. a: The maximum number of lamellae seen in the olfactory array of a particular species is given to the nearest decimal in brackets. b: These assignments are tentative. See Sections 5 and 8. c: If known, the length of cilia is indicated in brackets. d: Numbers in column indicate number of accessory sacs present. The olfactory chambers with which these accessory sacs are associated all possess a valve of some kind. NSE: Kinociliated cells are present within the non-sensory epithelium *only*. SE: Kinociliated cells are present in the sensory (*i.e.* olfactory) epithelium, but may also be present in the non-sensory epithelium. [•]: fish suggested for hydrodynamics experiments. SN: possesses only a single nostril and a single olfactory chamber. V: In both the hagfish and sea lamprey a valve prior to the olfactory chamber is believed to direct flow into the spaces between the olfactory lamellae (Theisen 1980, p. 280; Kleerekoper & van Erkel 1960, p. 215). S: possesses only a single nostril. R: Lamellae arranged in a radial fashion.

Table 2. Fluid dynamic data, including Reynolds and Péclet numbers, for flow within the olfactory lumen of three species of fish at 25 °C.

SHORT TITLE: Hydrodynamic aspects of fish olfaction

APPENDIX A

A.1. General methods

Live specimens of the bichir and blackspotted puffer mentioned in Section 3 and the sterlet mentioned in Section 5 were observed at Bristol Zoo Gardens, UK. A video clip of the trembling behaviour of the olfactory flaps of the blackspotted puffer is available at http://www.bath.ac.uk/chemistry/people/cox/puffer.html. The behaviour involves the flaps of the right-hand organ and occurs 1 s and 9 s into the clip.

The preserved specimens of the pike, garpike, angler fish (*Linophryne* species), haddock, longnose gar, broad-nosed pipefish are in the Natural History Museum, London, UK. The plan view of figure 5*c* was based on the right-hand olfactory organ of a recently dispatched European eel provided by the Environment Agency (Lower Severn Area Office, Tewkesbury, UK). The preserved specimen of the eel mentioned in Section 3 is in the teaching laboratory in the Department of Biology and Biochemistry, University of Bath, UK.

The dimensions of the olfactory organs of fish were estimated from diagrams in the literature using the software package Rhinoceros (Version 3.0, Robert McNeel & Associates) as follows. Lengths, surface areas and cross-sectional areas were calculated by importing a scan of the relevant diagram or photograph into a Rhinoceros file as a bitmap image (View menu: Background Bitmap → Place) and then using the appropriate tools to draw lines (for measuring lengths) or curves (to trace a feature whose area is required). Lines were drawn with the Line command (Curve menu: Line → Single Line). Outlines were drawn with the Free-Form command (Curve menu: Free-Form → Control Points). The length of a line was calculated using the Length command (Analyze menu: Length). Outlines were converted to planar surfaces using the Planar Curves command (Surface menu: Planar Curves), and the area of this surface measured using the Mass Properties command (Analyze menu: Mass Properties → Area). Lengths and areas estimated from bitmap images were converted to actual lengths and areas from the length of a diagram's scale bar.

The kinematic viscosity (υ) of fresh water at 25 °C was calculated using the equation (Vogel 1994, p. 25):

$$\upsilon = \frac{\mu}{\rho}$$

where μ and ρ are the dynamic viscosity and density of the fluid, respectively. At 25 °C the dynamic viscosity of fresh water is 0.89 x 10^{-3} Pa s (Lide 2004, section 6-203) and its density is 997 kg m^{-3} (Denny 1993, figure 4.3); thus its kinematic viscosity at this temperature is 0.89 x 10^{-6} m^2 s^{-1}. The kinematic viscosity and density of seawater (salinity 35 ‰) at 10 °C are 1.35 x 10^{-6} m^2 s^{-1} (Denny 1993, p. 63) and 1,027 kg m^{-3} (Denny 1993, p. 24), respectively.

Compounds known to elicit an olfactory response in fish (i.e. odorants) include amino acids (*e.g.* Theisen *et al.* 1991), steroids and prostaglandins (*e.g.* Bjerselius & Olsén 1993). Diffusion coefficients of molecules in this size range (relative molecular mass 100 - 500) at infinite dilution in water at 25 °C are *ca*. 10^{-9} m^2 s^{-1} (Table 5.2-1 of Cussler 1997).

Swimming speeds, based upon data in Table I of Beamish (1978), which lists sustained cruising speeds of migrating fish, were assumed to be 1 L s^{-1}, where L is the length of the fish.

Of the fish considered below, the haddock, blackspotted puffer, hardhead sea catfish, starry flounder and garpike live in a marine environment; the channel catfish, striped panchax and green swordtail are freshwater fish. The temperature of sea water is assumed to be 10 °C. The temperature of the freshwater environment inhabited by the striped panchax and green swordtail, both tropical fish, is assumed to be 25 °C. The temperature of the freshwater environment inhabited by the channel catfish is also assumed to be 25 °C.

A.2. Crude estimates of the thickness of the boundary layer of swimming fish

The thickness of the boundary layer (δ) at the anterior nostril of a haddock, or in the vicinity of the olfactory organ of a blackspotted puffer, was estimated using the equation (Vogel 1994, p. 158):

$$\delta = 5\sqrt{\frac{x\upsilon}{U}} \qquad \text{(A.2)}$$

where x is the distance downstream from the leading edge of a flat plate oriented parallel to the flow, υ is the kinematic viscosity of the fluid, and U in this case is the speed at which the fish swims. This equation assumes that flow is laminar, and that the fish are flat plates, which of course they are not, hence these estimates should be regarded as somewhat crude.

The distance from the tip of the snout to either anterior nostril in a preserved specimen of a haddock was 11 mm. The total length of this specimen was 22 cm, giving a swimming speed of *ca*. 0.2 m s^{-1}. Therefore δ = 1.4 mm at 10 °C.

The distance from the tip of the snout to either olfactory organ in a live specimen of a blackspotted puffer was estimated to be 20 mm. The total length of this specimen was *ca*. 20 cm, giving a swimming speed of 0.2 m s^{-1}. Therefore δ = 1.8 mm at 10 °C.

A.3. Diffusion times

Diffusion times (t) were calculated using the equation (Berg 1983, p. 10):

$$t = \frac{x^2}{2D} \qquad \text{(A.3)}$$

where x is the distance over which the species must diffuse and D is the diffusion coefficient (taken to be 10^{-9} m^2 s^{-1} – see Appendix A.1). In the case of diffusion times in the olfactory lumen, x is half the lumen depth.

A.4. Depth of the olfactory lumen of the channel catfish

The depth of the olfactory lumen of the channel catfish was estimated to be 10 – 70 μm from the following micrographs: figure 1*d* of Ngai *et al.* 1993; figures 2*c* and 3*a* of Morita & Finger 1998; figures 5*a* and 5*b* of Hansen *et al*. 2003.

A.5. Pressure difference between the anterior and posterior nostrils of the hardhead sea catfish

The dynamic pressure just in front of the anterior nostril of the hardhead sea catfish may be estimated from the equation $\frac{1}{2}\rho U^2$ (Vogel 1994, p. 53), where ρ is the density of the fluid, here seawater at 10°C, and U is the speed at which the fish swims. The fish described in Zeiske *et al.* 1994 were about 20 – 30 cm. Therefore U = 0.2 – 0.3 m s^{-1}, giving a dynamic pressure of 21 – 46 Pa. Assuming that the dynamic pressure at the posterior nostril is zero, this range also corresponds to the pressure difference across the chamber.

A.6. Estimates of Reynolds and Péclet numbers

Reynolds and Péclet numbers were calculated using equations 6.1 and 7.1. Both are quoted to one significant figure (Vogel 1994, p. 85).

A.6.1. Flow through the olfactory lumen of the striped panchax

In order to calculate Reynolds and Péclet numbers for flow through the olfactory lumen, one needs to know the average velocity of the flow in the lumen.

In the case of the striped panchax, this was calculated from measurements of the velocity of flow at the entrance of the anterior nostrils of the striped panchax and green swordtail made by Kux *et al.* (1978) using laser Doppler velocimetry, with the fish *stationary*. The maximum velocities here were found to be either 12 or 17 mm s^{-1} (which velocity is associated with which species of fish is not stated).

Using these figures, and estimates for the cross-sectional area of the anterior nostril and the olfactory chamber, one may, using the principle of continuity (Vogel 1994, pp. 32-34), calculate a range for the average velocity in the olfactory chamber.[5]

[5] The principle of continuity is valid only if the fluid is incompressible (Vogel 1994, p. 32). Water may be regarded as incompressible provided flow speeds are less than 1500 m s^{-1} (Vogel 1994, p. 21). Since flow speeds in the olfactory chambers of fish are much less than this, one may assume that the water in the chambers is incompressible and that the principle of continuity can be applied.

The cross-sectional area of the anterior nostril (a small tubular projection) of the striped panchax was estimated by measuring the diameter at its tip from figure 4*a* of Zeiske 1974 (right-hand nostril only – it is difficult to gauge the diameter of the left hand nostril) or from figure 1 of Kux *et al.* 1978, and then assuming the nostril is circular at this point. The former measurement gives a cross-sectional area of 0.03 mm^2, the latter 0.09 mm^2. These estimates are roughly in agreement with the (elliptical) cross-sectional area of 0.02 mm^2 that may be calculated assuming that the anterior nostril has "dimensions of less than 0.25 mm by 0.1 mm" (Kux *et al.*, 1977, p. 492).

The cross-sectional area of the olfactory chamber of the striped panchax was estimated from figure 3*c* of Zeiske 1974 to be 0.02 mm^2 (total length of fish 70 mm). The fact that there are three ridges on the floor of the chamber suggests, on consulting figure 4*a* of Zeiske 1974 (right-hand olfactory organ), that this cross-section was taken towards the rear of the chamber.

From the principle of continuity, (0.03 to 0.09 mm^2) x (12 or 17 mm s^{-1}) = 0.02 mm^2 x u, where u is the range of average velocities in the olfactory lumen. Therefore u = 18 – 77 mm s^{-1}.

The depth of the olfactory lumen of the striped panchax was estimated from figure 3*c* of Zeiske 1974 to be 13 – 43 μm. Thus the Reynolds number for flow in the olfactory lumen of the striped panchax is 0.3 to 4 at 25 °C. The Péclet number is 200 to 3,000 at 25°C.

With respect to these estimates, it should be noted that a) the cross-sectional area of the anterior nostril was estimated from figures (Zeiske 1974, figure 4*a* and Kux *et al.* 1978, figure 1) in which the length of the fish is not stated; and b) the length of the fish used to estimate the depth and cross-sectional area of the lumen (70 mm) is slightly different from the length of fish used to perform the laser Doppler velocimetry measurements (60 mm; Kux *et al.* 1978). Ideally, for a self-consistent estimate, all the data should come from the same fish. It should also be noted that these estimates were made assuming that the cross-sectional area of the olfactory

chamber does not change with the pumping action of the accessory sac, which may not be the case.

A.6.2. Flow through the olfactory lumen of the green swordtail

As for the striped panchax, the average velocity in the lumen of the green swordtail was estimated from laser Doppler velocimetry measurements (Kux *et al.* 1978) at the anterior nostril using the principle of continuity. The maximum velocity at the anterior nostril was either 12 or 17 mm s^{-1} (Appendix A.6.1).

The cross-sectional area of the anterior nostril of the green swordtail can be estimated from the inner and outer rims of the entrance shown in figure 4*a* of Kux *et al.* (1988). The area bounded by inner rim is 0.01 mm^2 and the area bounded by outer rim is 0.02 mm^2, giving a range of 0.01 – 0.02 mm^2. However, it should be noted that: a) the section through this entrance, based on a comparison with figure 1 of Zeiske (1974), is likely to be oblique and b) based on a comparison with figure 6 of Zeiske (1973), the fish whose olfactory chamber is shown in figure 4*a* of Kux *et al.* (1988) is between 33 – 46 mm in total length, and thus smaller than the fish used for the laser Doppler velocimetry study (60 mm). Both these points suggest that the cross-sectional area of the anterior nostril will be an underestimate.

The cross-sectional area of the olfactory chamber can be estimated from figure 3 of Zeiske (1973) as 0.03 mm^2. The size of the fish that gave rise to the cross-section shown in this figure, and the region of the olfactory chamber from which it was taken, are not stated in this figure legend.

Using the cross-sectional areas of the anterior nostril and olfactory chamber of the green swordtail, together with the maximum velocities at the anterior nostril, the average velocity in the olfactory lumen may, again from the principle of continuity, be calculated as 4 - 11 mm s^{-1}. Note that this range is, as the cross-sectional area of the anterior nostril was probably underestimated, probably also an underestimate.

The depth of the olfactory lumen of the striped panchax was estimated from figure 3 of Zeiske (1973) to be 21 – 69 μm. Thus the Reynolds number for flow in the

olfactory lumen of the green swordtail is 0.09 to 0.9 at 25 °C. The Péclet number is 80 to 800 at 25 °C. Given that the range of average velocities in the olfactory lumen may be underestimated, these figures for *Re* and *Pé* may also be underestimated.

A.6.3. Flow through the olfactory lumen of the channel catfish

The depth of the olfactory lumen of the channel catfish is 10 – 70 μm (Appendix A.4). The average velocity of the fluid in the lumen may be taken to be 2 mm s^{-1} (Section 6). Thus the Reynolds number for flow in the olfactory lumen of the channel catfish is 0.02 to 0.2 at 25 °C. The Péclet number is 20 to 100 at 25 °C.

A.6.4. Flow through the olfactory chamber of the starry flounder

The range of Reynolds numbers (300 – 600) for flow through the olfactory chamber of the starry flounder given in Section 6 deviates slightly from the range of 100 – 1,000 stated by Nevitt (1991, p.15). The range given in Section 6 was calculated as follows. Nevitt estimates that the volume change in the olfactory organ accompanying a coughing event is 310 mm^3 ("0.03-0.34 ml"), and that this change takes 0.25 s. Thus the flow rate into the chamber is 1,240 mm^3 s^{-1}. From her estimate of the cross-sectional area of the chamber (3 – 7 mm^2), the average velocity in the chamber is about 0.2 – 0.4 m s^{-1}. From her figures for the average velocity in the chamber (0.06 – 0.6 m s^{-1}) and the Reynolds numbers for flow within the chamber (100 – 1,000), the characteristic length she used to obtain the latter may be inferred to be about 2 mm at 10 °C. From this figure, and u = 0.2 – 0.4 m s^{-1}, the Reynolds number for flow within the chamber at 10 °C may be estimated to be 300 – 600. Nevitt's figures of 0.06 – 0.6 m s^{-1} for the average velocity in the olfactory chamber appear to have been derived (erroneously) from the flow rate into the chamber (1,240 mm^3 s^{-1}) and her estimate of the cross-sectional area of the anterior nostril of the olfactory organ (0.2 – 1.8 mm^2): together these figures actually give an average velocity of 0.7 – 6 m s^{-1}, not the range of 0.06 – 0.6 m s^{-1} stated by Nevitt (1991, p. 15).

A.6.5. Flow in the duct leading from the accessory sac to the posterior nostril of the striped panchax

Maximum velocities at the posterior nostril of the striped panchax and green swordtail were found to be 30 and 35 mm s^{-1} using laser Doppler velocimetry, with the fish

stationary (Kux *et al.* 1978) (again which velocity is associated with which species of fish is not stated). The cross-sectional area of the posterior nostril of the striped panchax was estimated to be 0.02 – 0.05 mm^2 from figure 1 of Kux *et al.* (1978) (length of fish not stated). The cross-sectional area of the accessory sac duct where it passes the back of the olfactory chamber may be estimated to be 0.1 mm^2 from figure 4*a* of Zeiske 1974. Using the principle of continuity, the average velocity of flow in the accessory sac duct as it passes the rear of the olfactory chamber may therefore be estimated to be 6 – 18 mm s^{-1}. From figure 4*a* of Zeiske (1974), the width of the accessory sac duct at this point is 0.5 mm. Therefore the Reynolds number in the accessory sac duct at this point is 3 to 10 at 25 °C.

A.6.6. Flow directly above the olfactory pit of a garpike

Adult garpike can attain lengths up to 76 cm (Wheeler 1969, p. 236), giving a swimming speed of *ca*. 0.8 m s^{-1}. However, given that garpike can swim fast (Theisen *et al.* 1980, p. 169), one may reasonably assume a swimming speed of 1 m s^{-1}. Each side of the triangular olfactory pit shown in figure 3 is about 7 mm. This is the characteristic length of the pit. The Reynolds number at 10 °C is therefore 5,000.

A.6.7. Flow around the olfactory organs of the blackspotted puffer

The characteristic length of the olfactory organ of a blackspotted puffer is its greatest length in the direction of flow (Vogel 1994, p. 85), here about 3 mm. The length of an adult blackspotted puffer is about 20 cm, giving a swimming speed of 0.2 m s^{-1}. The Reynolds number at 10°C is therefore about 400.

A.7. Power required to pump water through the olfactory chamber of a starry flounder

The power (P) required to pump fluid through a duct is given by the equation $P = Q\Delta p$, where Q is the flow rate through the duct and Δp is the pressure difference across the duct (Vogel 1994, p. 324). Therefore to calculate the power required to pump water through the olfactory chamber of a fish, one needs to know the flow rate through the olfactory chamber and the pressure change generated across the chamber by the pumping mechanism.

The following calculations make use of data presented primarily in figure 3*a* of Nevitt (1991), which gives masses of latex casts of the eyed-side olfactory organ (olfactory chamber and two accessory sacs) of several different specimens of starry flounders. (Note that the ordinate units in this figure should be mg, not g.) The casts were taken with the flounders' jaws fixed in either an abducted position (*i.e*. with the mouth open, as it would be at regular intervals during the course of normal respiration), or in a protruded ("coughing") position. Specifically the calculations make use of the masses of the casts taken from a pair of starry flounders with an "eye-pectoral fin distance" of about 55 mm. Based on pictures of starry flounders (*e.g.* Norman 1934, p. 384), each of these specimens would have a standard length of *ca.* 27 cm. The mass of a starry flounder of standard length 27 cm may be estimated, using the data of Orcutt (1950, figure 50), to be 500 g. Masses of casts were converted to volumes using a density for natural latex of 0.95 g cm^{-3} (Carolina Biological Supply, personal communication) at 25 °C. The calculations make a number of assumptions, and should therefore be regarded as crude at best.

The pressure change generated by the pumping action of the two accessory sacs of a starry flounder during normal respiration is about 25 Pa (Nevitt 1991, p. 8). The flow rate through the olfactory chamber may be estimated as follows. From figure 3*a* of Nevitt (1991), the volume of the eyed-side olfactory organ of a *ca.* 27 cm starry flounder in an abducted position (*i.e*. with the accessory sacs expanded) is about 20 mm^3. The volume of the chamber is assumed to be negligible with the mouth closed. The respiratory cycle of a flatfish is 1 – 3 s (Hughes 1960, p. 38; Kerstens *et al*. 1979, p. 172; Steffensen *et al.* 1982, Table 1). Assuming that expansion of the accessory sacs takes half this time (and probably more: Nevitt 1991, p. 8), the flow rate into the chamber may be estimated to be about 10 – 40 $mm^3\ s^{-1}$. Therefore the power required to pump water through the olfactory chamber during normal respiration is, using $P = Q\Delta p$, about 0.25 – 1 μW.

The pressure change accompanying a cough in the starry flounder is about 140 Pa (Nevitt 1991, figure 2). From figure 3*a* of Nevitt (1991), the volume of the eyed-side olfactory organ of a *ca.* 27 cm starry flounder in a protruded position (*i.e.* presumably with the accessory sacs greatly expanded) is about 170 mm^3. From figure 2 of Nevitt

(1991), the time taken for the pressure to fall in the nasal cavity during a cough is about 0.2 s. Therefore the flow rate into the chamber during the cough, assuming that the volume of the chamber is negligible at the beginning of the cough, is about 850 $mm^3\ s^{-1}$. The power required to pump water through the olfactory chamber during a cough is therefore about 0.1 mW.

The average oxygen uptake for resting flounder, *Platichthys flesus*, in the size range 150 – 550 g at 8 – 10 °C is 0.45 ml O_2 per kg of body mass per minute (Kerstens *et al.* 1979). Whilst this is not the average oxygen uptake for a resting starry flounder (there is no value in the literature for a specimen of 500 g), the size range of the specimens for which it was calculated does incorporate 500 g specimens, and *Platichthys flesus* and the starry flounder (*Platichthys stellatus*) belong to the same genus. Thus this figure might be reasonably used to estimate the resting metabolic rate of a 500 g starry flounder. Since 1 ml of O_2 is equivalent to an energy expenditure of 20 J (Schmidt-Nielsen 1998, p. 194), the resting metabolic rate of this specimen would be about 0.1 W.

Thus power required to pump water through the olfactory chamber during normal respiration is 0.00025 - 0.001 % of the resting metabolic rate of a flounder, and during a cough is 0.1 % of this resting metabolic rate.

Appendix B

English common name[a]	Current scientific name[b]	Previous scientific name(s)[c]
Ribbon moray	*Rhinomuraena quaesita*	*Rhinomuraena ambonensis*
Puffer	*Takifugu pardalis*	*Tetraodon pardalis, Fugu pardale*
Northern puffer	*Sphoeroides maculatus*	*Spheroides maculatus*
Blackspotted puffer	*Arothron nigropunctatu*s	*Tetraodon nigropunctatu*s
Spotted sorubim	*Pseudoplatystoma corruscans*	*Playstoma coruscans*
Mexican barred snapper	*Hoplopagrus guentherii*	*Hoplopagrus guentheri*
Cave fish	*Astyanax jordani*	*Anoptichthys jordani*
Great snakehead	*Channa marulius*	*Ophiocephalus marulius*
Spotted snakehead	*Channa punctata*	*Channa punctatus*
Green swordtail	*Xiphophorus hellerii*	*Xiphophorus helleri*
Hardhead sea catfish	*Ariopsis felis*	*Arius felis*
Reedfish	*Erpetoichthys calabaricus*	*Calamoichthys calabaricus*
Flounder	*Platichthys flesus*	*Pleuronectes flesus*
Jarbua terapon	*Terapon jarbua*	*Therapon jarbua*
Macculloch's rainbowfish	*Melanotaenia maccullochi*	*Nematocentris maccullochi*
Red piranha	*Pygocentrus nattereri*	*Serrasalmus nattereri*

a: As given in FishBase (http://www.fishbase.org/search.php).
b: As given in California Academy of Sciences's *Catalog of Fishes* (http://www.calacademy.org/RESEARCH/ichthyology/catalog/fishcatsearch.html).
c: *i.e.* Name(s) given in literature cited.

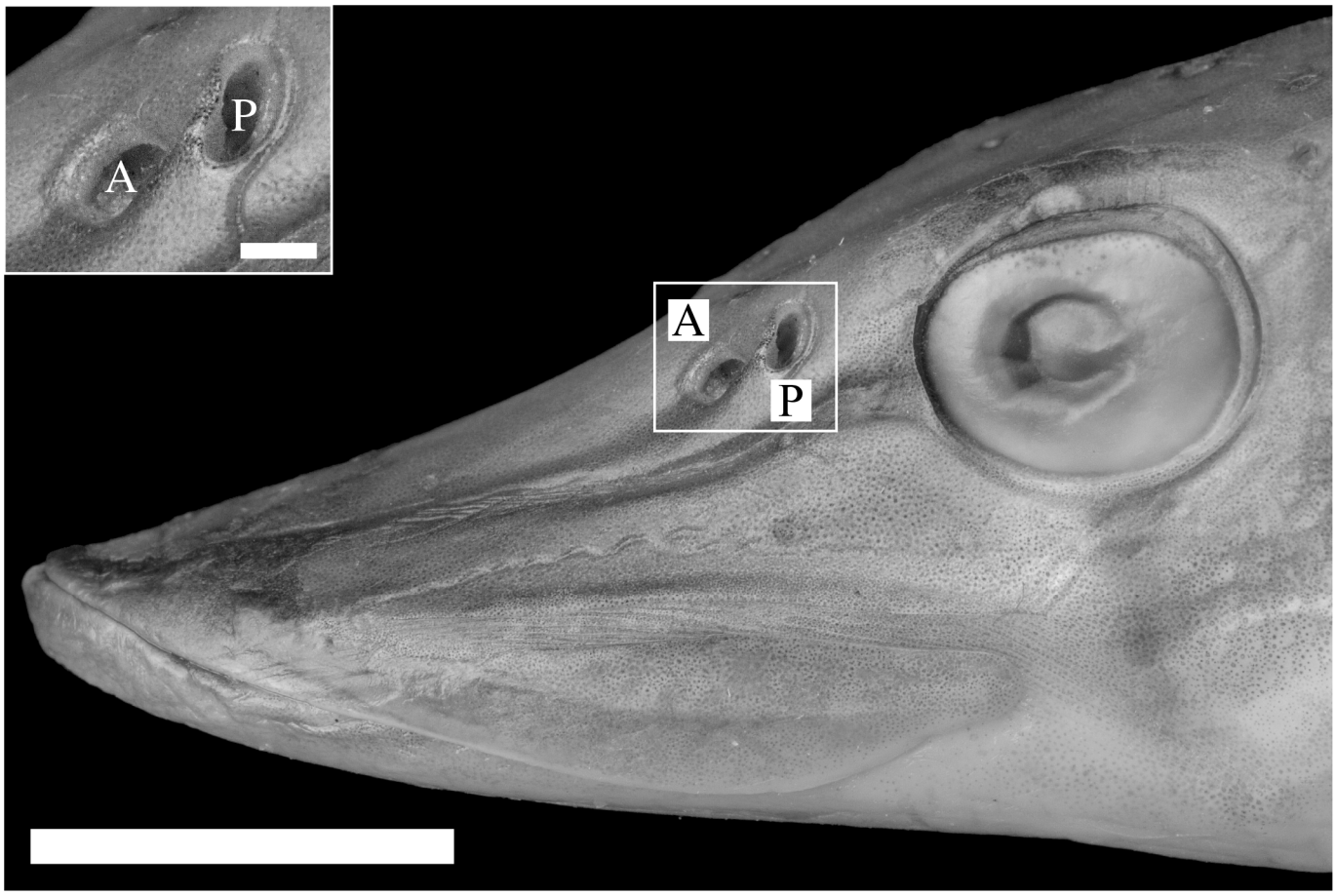

Figure 1. Photograph of the head of a preserved Northern pike (*Esox lucius*) specimen (total length 17 cm), lateral (left-hand side) aspect. Boxed region highlights the anterior (A) and posterior nostrils (P). Scale bar: 1 cm. Inset: boxed region from main photograph. Scale bar 1 mm. Photograph copyright Natural History Museum, London (specimen catalogue number BMNH 1963.4.26:1-2).

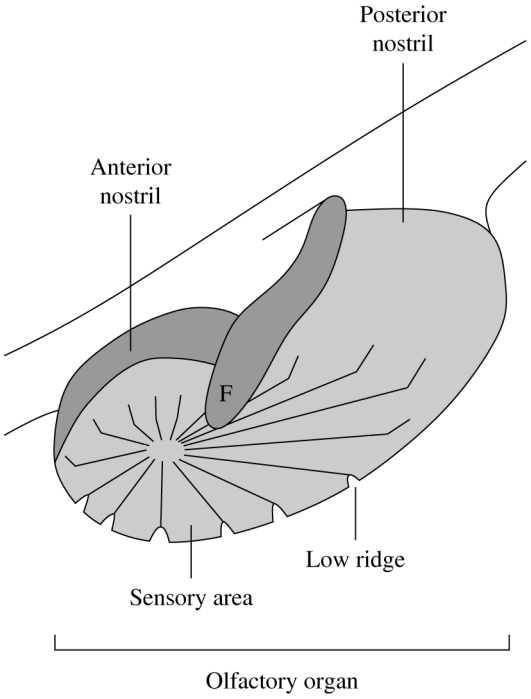

Figure 2. Schematic showing the main features of the olfactory organ of a Northern pike (longitudinal cross-section). The olfactory chamber is shaded light grey. This particular chamber includes an internal flap (F) believed to direct flow onto the sensory area (Burne 1909, p. 629). The latter is located between the low ridges, and at the centre of the radial arrangement formed by the ridges. In fact, the ridge system is more complicated than shown, with minor ridges lying between major ridges, and transverse ridges connecting the major and minor ridges, giving a cobweb-like structure, with the sensory region occupying the spaces in the cobweb (Holl 1965, pp. 738-740). Schematic based on Text-fig. 198 of Burne (1909) and figure 21 of Teichmann (1954).

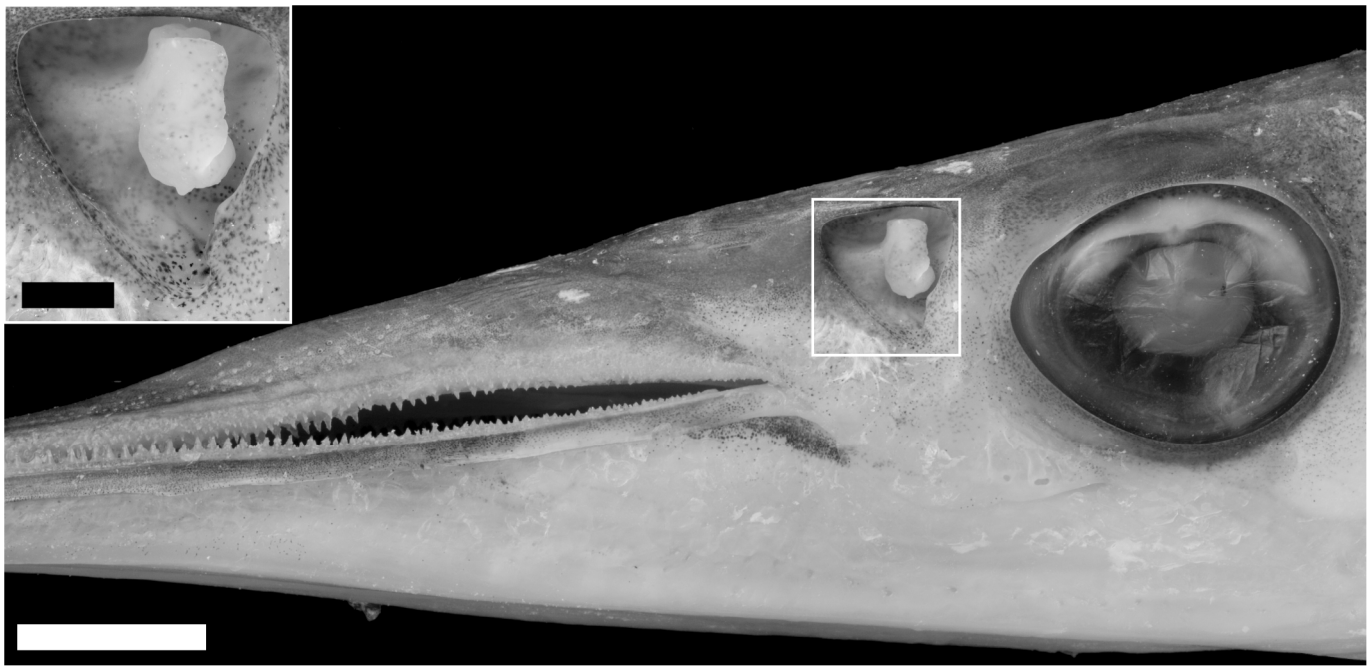

Figure 3. Photograph of the preserved head of a garpike, *Belone belone*, highlighting the triangular olfactory pit (boxed region). The olfactory epithelium coats both boss and pit (Theisen *et al.* 1980, figure 2*d*). Scale bar: 1 cm. Inset: boxed region from main photograph. Scale bar: 250 μm. Photographs copyright Natural History Museum, London (specimen catalogue number BMNH 2005.4.27:24-30).

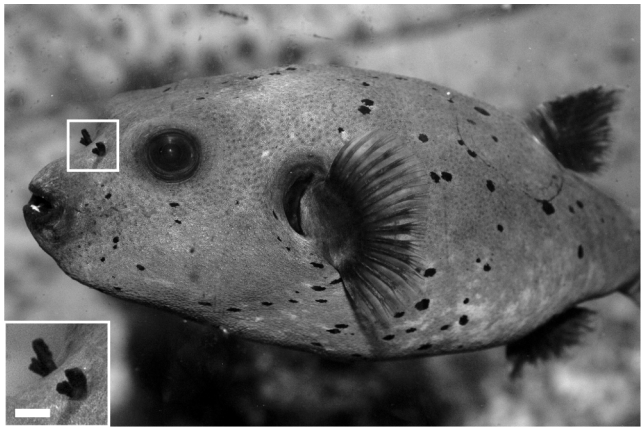

Figure 4. Photograph of a live blackspotted puffer, *Arothron nigropunctatu*s (normal phase). The olfactory organs are the pair of dark, forked structures lying within the boxed region. Inset: boxed region from main photograph. Scale bar *ca.* 3 mm. Photograph courtesy of Bristol Zoo Gardens, UK.

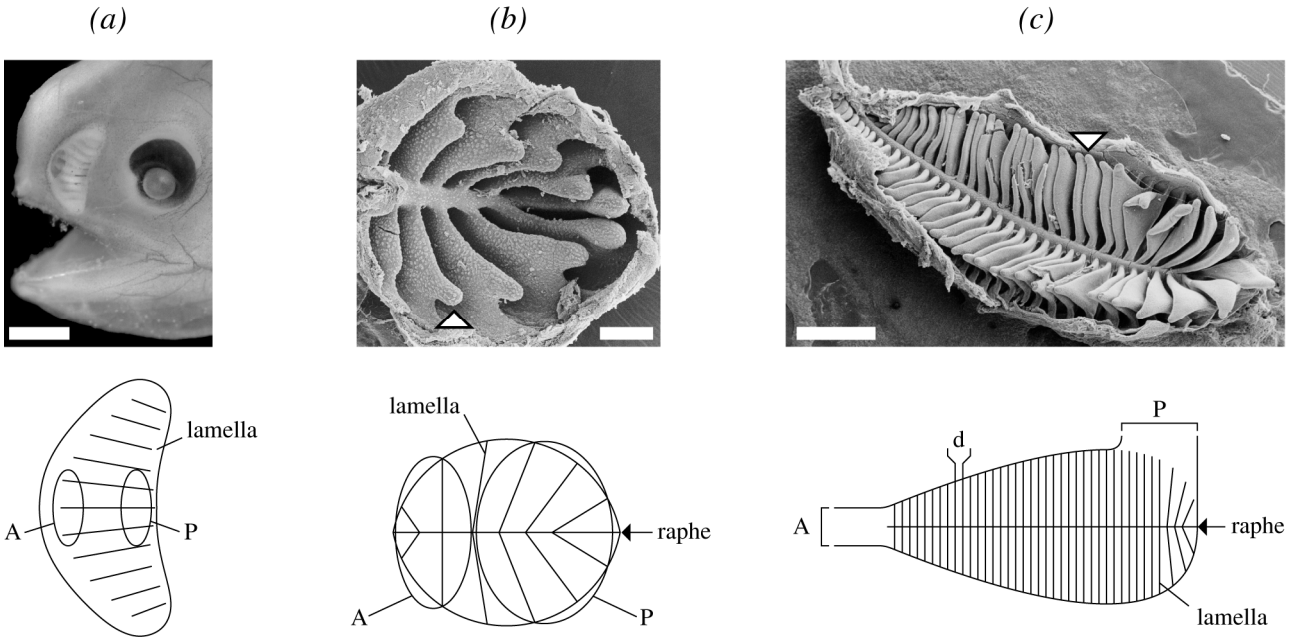

Figure 5. Three different types of olfactory lamellar array. (*a*) Longitudinal array of olfactory lamellae. Top: photograph of lateral aspect of head of a preserved specimen of a male angler fish (*Linophryne* species, total length 22 mm). Photograph copyright Natural History Museum, London (specimen catalogue number BMNH 2004.11.6.44). Bottom: plan view of olfactory chamber. Scale bar: 1 mm. *(b)* Rosette. Top: electron micrograph of olfactory chamber of goldfish, *Carassius auratus*. Reprinted with permission of Wiley-Liss, Inc., a subsidiary of John Wiley & Sons, Inc. from Hansen *et al.* (2004). Copyright 2004 John Wiley & Sons, Inc. Scale bar: 0.3 mm. Bottom: plan view. *(c)* Elongated rosette. Top: electron micrograph of olfactory chamber of European eel, *Anguilla anguilla*. Note that the raphe is gently curved rather than straight. Scale bar: 1 mm. Reproduced with permission of Springer Science + Business Media, LLC from Hansen & Zielinski (2005). Copyright 2006 Springer Science + Business Media, LLC. Bottom: Plan view of olfactory chamber. A and P: outlines/positions of anterior and posterior nostrils, respectively; d: distance between successive olfactory lamellae (referred to here as the depth of the olfactory lumen). The arrows in figures 5*b* and 5*c* highlight the rounded fin-like extremities of the lamellae, potential candidates for shedding tip vortices (Section 8).

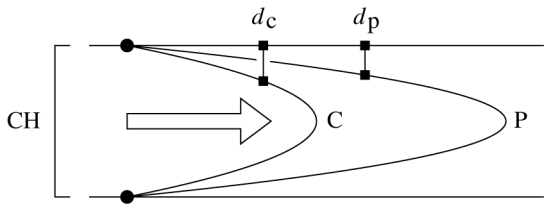

Figure 6. Comparison of velocity profiles for fully developed flow between two wide but closely spaced parallel plates (P) and within a circular pipe (C). Parabolic flow between the parallel plates is, on the average, closer to the walls of the channel (CH) than in a circular pipe, given that the channels are of the same length, the diameter of the circular pipe is equal to the perpendicular distance between the two parallel plates, and the fluid flowing through them has the same viscosity. The vertical lines below d_P and d_C show the average distances of the flow from the wall of the parallel plate channel and the circular pipe, respectively. Arrow: direction of flow. Filled circles indicate that the velocity at the wall is zero (the no-slip condition [Vogel 1994, pp. 18-20]).

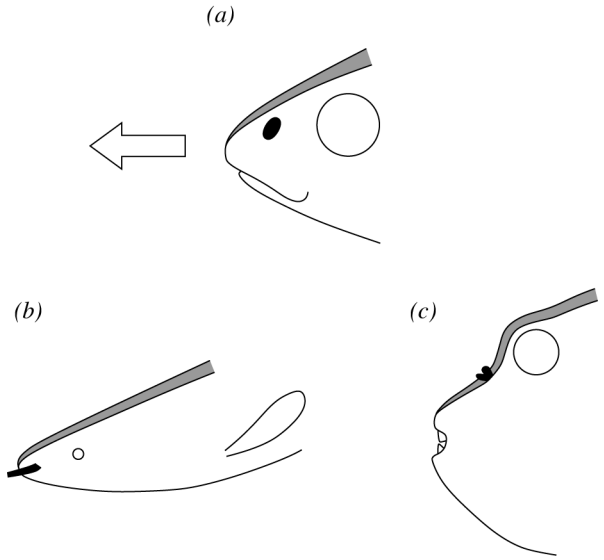

Figure 7. Boundary layers associated with swimming fish. The boundary layers indicated (shaded) are highly schematic, and are of course shown in two-dimensions only. The relative motion of the fish with respect to the water (arrow) in each case is from right to left. *(a)* Profile of the head of a haddock (*Melanogrammus aeglefinus*) from a drawing (Wheeler 1969, p. 277). Approximate location of olfactory organ indicated by the filled oval. *(b)* Profile of the head of a bichir (*Polypterus endlicheri*) based on video footage of a swimming fish at Bristol Zoo Gardens, UK. Only the left-hand tubular anterior nostril is apparent (black). *(c)* Profile of head of blackspotted puffer taken from video footage of a swimming fish at Bristol Zoo Gardens, UK. Only the left-hand olfactory organ is apparent (black). Diagrams not to scale.

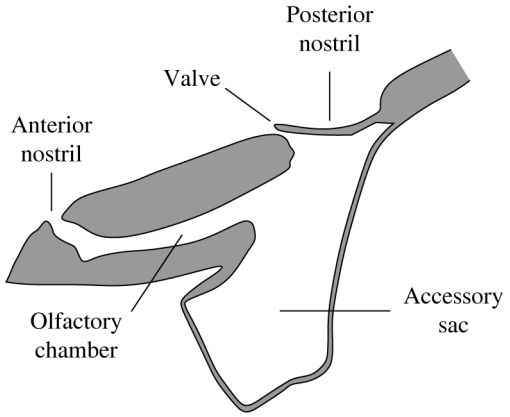

Figure 8. Schematic longitudinal cross-section through the olfactory organ of an "oviparous cyprinodont" fish (Zeiske 1974), a group to which the striped panchax belongs. Based on figure 3*a* of Kux *et al.* 1988, the same cross-section through the green swordtail is likely to be similar. Figure redrawn from figure 1 of Zeiske 1974.

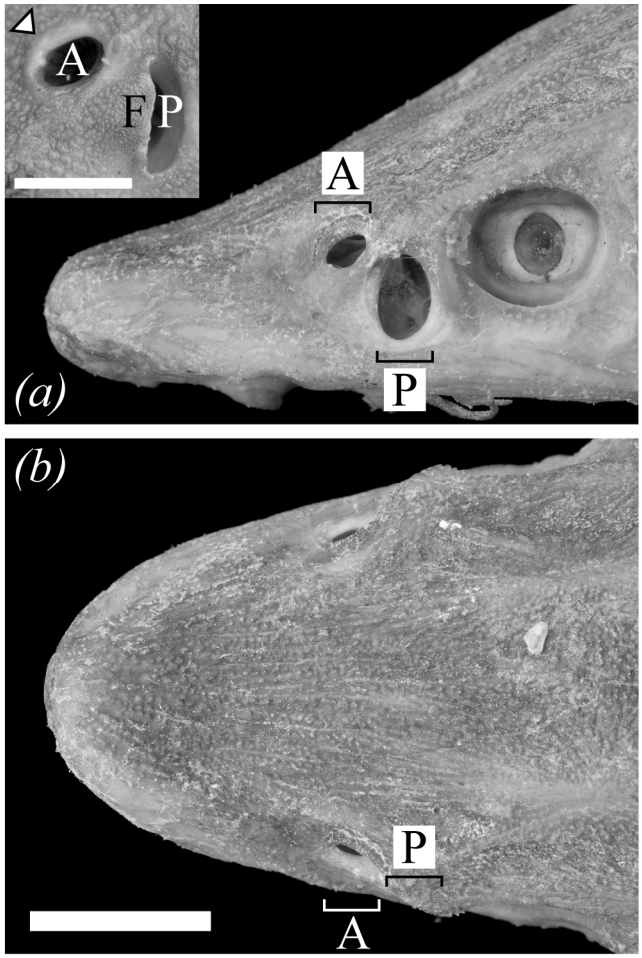

Figure 9. Main pictures: photographs of the head of a preserved specimen of a sterlet, *Acipenser ruthenus* (total length *ca.* 35 cm). *(a)* Lateral view, showing anterior and posterior nostrils of left-hand olfactory organ. Inset: photograph of the anterior and posterior nostrils of the olfactory organ of a lake sturgeon, *Acipenser fulvescens* (total length *ca*. 25 cm), highlighting the well-rounded rim of the anterior nostril (arrowhead). The posterior nostril of this particular organ is, unusually for sturgeons, partially occluded by a flap of skin (F); the posterior nostril of the other olfactory organ of this specimen was the more typical oval hole. Scale bar: 5 mm. (*b*) Dorsal view. Note the protruding posterior nostril. Scale bar: 1 cm. Scale for both (*a*) and (*b*) is the same. A: anterior nostril; P: posterior nostril. Photographs courtesy of the Natural History Museum [specimen catalogue numbers BMNH 1896.10.3.53-54 (*Acipenser ruthenus*) and BMNH 1963.10.28.5 (*Acipenser fulvescens*)].

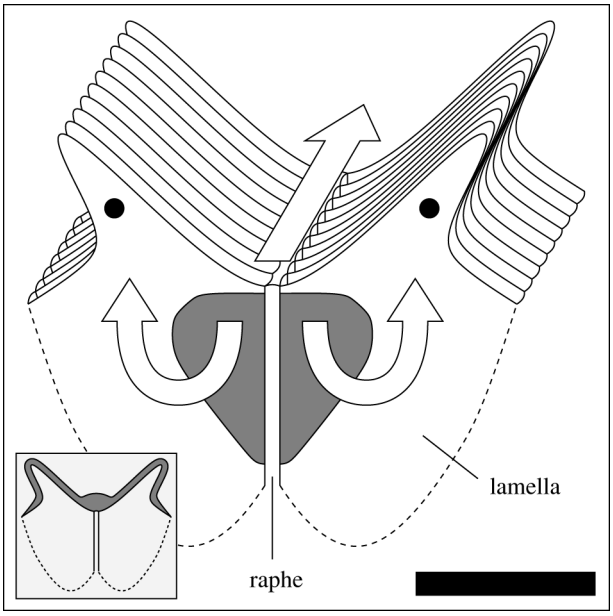

Figure 10. Schematic of part of the elongated olfactory rosette of the channel catfish, *Ictalurus punctatus*. Lamellae are attached to the raphe, and to the floor and sides of the olfactory chamber (dotted lines). The roof of the chamber is not shown in the main picture but is shown in the inset. The free edges of the lamellae protrude into the channel (grey in inset) above the array. There is no information in the literature on the nature of this channel, though based on the anatomy of other fish with similar olfactory organs (*e.g*. the European eel [Teichmann 1959, p. 241] and the catfish *Wallago attu* [Ojha & Kapoor 1972, pp. 108-110]), the channel is probably narrow. The arrow above the array indicates the direction of flow in this channel. The sensory areas of the two nearest lamellar faces are shown in grey (only the sensory area on the nearest pair of lamellar faces is shown, for convenience); the remaining lamellar area is predominantly occupied by kinociliated cells. The curved arrows indicate the approximate direction of flow over the lamellae. Again, there is no information in the literature on the direction of flow over the olfactory lamellae of the channel catfish, and the direction shown here is an assumption based on the location of the kinociliated cells. Flow is only shown on the nearest pair of lamellar faces, but will be similarly directed over the other lamellar faces in the array. The fin-like dorsal regions (filled circles) of each lamella are potential candidates for shedding tip vortices (Section 8). Scale bar: 0.5 mm. The schematic is based on figure 1 of Erickson & Caprio 1984.

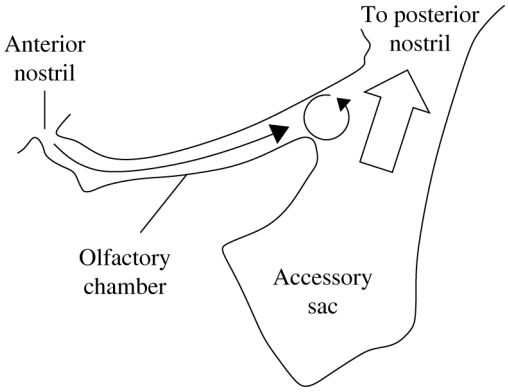

Figure 11. Schematic showing how water expelled from a single accessory sac (large arrow) could cause a vortex (circular arrow) at the back of the olfactory chamber of a fish, leading to enhanced odorant transfer and possible entrainment of fluid through the anterior nostril (long arrow). Adapted from figure 1 of Zeiske 1974. See also figure 8.

Fish	Lamellar array[a]	Externally induced flow[b]	Channeling agent(s)	Beating of cilia[c]	Accessory sac[d]	Other mechanisms	Principal reference(s)
Garpike, *Belone belone* [•]	Boss	Vortex					Theisen *et al.* 1980
Puffer, *Takifugu pardalis* [•]	Longitudinal (10)	Vortex					Wiedersheim 1887; Yamamoto & Ueda 1979a
Reedfish, *Erpetoichthys calabaricus*	Compound rosette (170)			NSE (10-20)			Pfeiffer 1968; Theisen 1970; Schulte & Holl 1971
European eel, *Anguilla anguilla*	Elongated rosette (90)			SE			Liermann 1933; Teichmann 1954, 1959; Holl 1965; Schulte 1972
Channel catfish, *Icatulurus punctatus* [•]	Elongated rosette (60)			NSE (15-20)			Caprio & Raderman-Little 1978; Cancalon 1978
Kidako moray, *Gymnothorax kidako*	Elongated rosette (130)			SE (15)			Yamamoto & Ueda 1978b
Ribbon moray, *Rhinomuraena quaesita*	Elongated rosette (110)			SE (15)			Holl *et al*. 1970
Hagfish, *Myxine glutinosa* (SN; V)	Longitudinal (10)					Respiratory flow	Theisen 1973
Striped eel catfish, *Plotosus lineatus*	Longitudinal (10)				1		Yamamoto & Ueda 1978c; Theisen *et al.* 1991
Striped panchax, *Aplocheilus lineatus*	-				1		Zeiske 1974; Zeiske *et al.* 1976
Green swordtail, *Xiphophorus hellerii*	-				1		Zeiske 1973; Zeiske *et al.* 1976
Sea stickleback, *Spinachia spinachia* (S)	-				1		Theisen 1982
Sea lamprey, *Petromyzon marinus* (SN; V) [•]	Longitudinal (30) R				1		Kleerekoper & van Erkel 1960
Common sole, *Solea solea* [•]	Elongated rosette (40)				"two-lobed"		Burne 1909; Holl 1965
Northern pike, *Esox lucius* [•]	See figure 2 of article	Venturi		NSE			Burne 1909; Teichmann 1954; Holl 1965
Sturgeon (*Acipenser* species) [•]	Radial (30)	Venturi		SE (10)			Bateson 1890; Chen & Arratia 1994; Zeiske *et al*. 2003
Goldfish, *Carassius auratus* [•]	Rosette (20)	Pitot	Flap	SE (10-12)			Yamamoto & Ueda 1978a; Hansen *et al*. 1999
Red piranha, *Pygocentrus nattereri*	Rosette (30)	Pitot	Flap	SE			Schulte & Riehl 1978
Tench, *Tinca tinca*	Rosette (30)	Pitot	Flap	SE			Burne 1909; Døving *et al*. 1977
Hardhead sea catfish, *Ariopsis felis*	Elongated rosette (40)	Pitot	Funnel	SE			Zeiske *et al.* 1994
Various sharks [•]	Elongated rosette (40)	Pitot	Channel, tube	SE		Respiratory activity	Theisen *et al.* 1986; Zeiske *et al.* 1987
European perch, *Perca fluviatilis*	Rosette (20)		Flap	SE	2		Burne 1909; Liermann 1933; Teichmann 1954; Holl 1965
European plaice, *Pleuronectes platessa* [•]	Longitudinal (30)		Hood	SE	2		Burne 1909; Holl 1965

Table 1

Fish	Primary means of ventilation	Lumen depth (μm)	Velocity (mm s^{-1})	*Re*	*Pé*
Striped panchax, *Aplocheilus lineatus*	Accessory sac	13 - 43	18 - 77	0.3 - 4	200 – 3,000
Green swordtail, *Xiphophorus hellerii*	Accessory sac	21- 69	4 - 11	0.09 - 0.9	80 - 800
Channel catfish, *Ictalurus punctatus*	Beating of cilia	10 - 70	2	0.02 - 0.2	20 - 100

Table 2